

# **3-Dimensional Mapping of Underwater Surface for Navigation Using Underwater Ultrasonic Piezoelectric Transducer**

Navan Tanjeem Hossain  
Rahat Mahmood Khan  
Saifur Rahman

Supervised by  
Dr. Md. Ziaur Rahman Khan  
Professor, Department of Electrical and Electronic Engineering,  
BUET, Dhaka-1000, Bangladesh.

A Thesis  
Submitted to the Department of Electrical and Electronic Engineering  
Of  
**BRAC University**

In partial fulfillment of the requirements for the degree of  
Bachelor of Science in Electrical and Electronic Engineering



April, 2017  
BRAC University, Dhaka

# 3-Dimensional Mapping of Underwater Surface for Navigation Using Underwater Ultrasonic Piezoelectric Transducer

Navan Tanjeem Hossain

Rahat Mahmood Khan

Saifur Rahman

April, 2017

BRAC UNIVERSITY

## DECLARATION

We hereby declare that the research work titled, “*3-Dimensional Mapping of Underwater Surface for Navigation using Underwater Ultrasonic Piezoelectric Transducer*” – is our own brain child except as cited in the text and in the reference section. This work has not been presented or submitted anywhere else for assessment or award of any degree or publication.

.....  
Dr. Ziaur Rahman Khan  
Thesis Supervisor  
Professor, Department of EEE, BUET.

.....  
Saifur Rahman  
13310001, ECE

.....  
Navan Tanjeem Hossain  
13121084, EEE

.....  
Rahat Mahmood Khan  
13121076, EEE

## ACKNOWLEDGEMENTS

Firstly, we would like to express our hearty gratitude to our Thesis Supervisor, Dr. Md. Ziaur Rahman Khan, Professor, Department of EEE, BUET for all the perseverance, guidelines and support that he has gifted us along the way completing the thesis. We are truly grateful to him for his patience and for believing in us.

We would also like to thank Mr. Abby Wang, Sales, CNIRHurricane Tech. (Shenzhen) Co. Ltd, China for dispatching the parcel of the transducers under the clock so we could get the transducers as soon as possible.

We would also like to sincerely thank Mr. Muhammad Sahool Afzal, The Registrar, BRAC University for authorizing the permission to receive the transducers that were stuck in Bangladesh Customs, Hazrat Shahjalal International Airport.

Further, we would also like to thank Dr. Md. Mosaddequer Rahman, Professor, Department of EEE, BRAC University for sprinkling quick suggestions from his vast knowledge of transducers when we approached him.

Furthermore, we would like to thank Dr. Md. Hasanuzzaman Sagor, Assistant Professor, Department of EEE, BRAC University and Mr. Avijit Das, Lecturer, Department of EEE, BRAC University for their quick suggestions on simulation software and being available when we sought help.

We would also like to thank, Saifur Rahman's Grand Father, Haji Md. Oziullah and Rahat Mahmood Khan's Uncle, Fuad Hossain for dispatching and managing few of the equipment's from UK.

Finally, we would like to thank each other. None of us alone could have accomplished the work. Working with the team was always a privilege. Hope our hard work pays off in helping solve the country's problem and we can provide more to the country and to the world.

## **ABSTRACT**

In the era of modern technology, even today, the underwater surface perception and mapping is still a much vague subject. Many approaches have been carried out following the topic. In a third world country, like Bangladesh, where water body is very important part of communication, life gets hindered when visual aids are compromised during navigation. The thesis conducted works to design a system to perceive and map the underwater surface. An underwater ultrasonic piezoelectric transducer has been chosen depending on the range to be perceived. A module has been designed from scratch to excite the transducer via a microcontroller unit and supply distances for mapping of the underwater surface. A program has also been developed to map the distances into a terrain and hereby display the distances in the form of 3-dimensional surface.

## ABBREVIATIONS

LAD – Least Available Depth

PZT – Piezoelectric Transducer

FOP – Frequency of Operation

SNR – Signal to Noise Ratio

TOF – Time of Flight

BW – Bandwidth

GPR – Ground Penetrating Radar

LIDAR – Light Detection And Ranging

AUV – Autonomous Underwater Vehicle

SfM – Structure from Motion

SWATH – Small Waterplane Area Twin Hull

MCU – Microcontroller Unit

MFB – Multiple Feed Back

DOF – Degree of Freedom

## List of Figures

Fig. no.	Title	Page no.
Fig 2.01:	Acoustic boundary reflection in different medium $Z_1$ & $Z_2$	15
Fig 2.02:	Transmitted and echo pulse	16
Fig 2.03:	MatLab polarpattern	17
Fig 2.04:	Electrical equivalent circuit of transducer	18
Fig 2.05:	Distance from multiple echo calculation	19
Fig.3.01:	Beam angle definition	22
Fig.3.02:	Transducer equivalent circuit (same as Butterworth impedance matching model)	24
Fig 4.01:	Block Diagram of Ultrasonic Transducer Communication System	26
Fig.4.02:	Ultrasonic Voltage Drive	27
Fig.4.03:	Oscillatory Circuit for 200 kHz generation (555 configuration)	27
Fig 4.04:	Oscilloscope View of 200 kHz generation	27
Fig.4.05:	Power Voltage Drive	28
Fig 4.06:	Single Stage Amplification	28
Fig.4.07:	Parallel Equivalent Circuit for modelling	29
Fig.4.08:	Maximum Power Transfer	29
Fig.4.09:	Series Resonance equivalent circuit	30
Fig.4.10:	L, C Value to match Transducer Impedance	31
Fig.4.11:	Power Vs Current/ Voltage Characteristics	32
Fig.4.12:	Impedance Matching	33
Fig.4.13:	Impedance Matching Circuit	33
Fig 4.14:	Generic Butterworth's 4 <sup>th</sup> Order Active Band-pass filter using MFB Topology	34
Fig.4.15:	Butterworth's 4 <sup>th</sup> Order Active Band-Pass filter using MFB topology	36
Fig.4.16:	Butterworth active Band pass filter using MFB topology	37
Fig.4.17:	Bode Plot and Phase Diagram of designed Filter	37
Fig.4.18:	Single Stage Peak detector	38
Fig.4.19:	Two-stage Peak detector circuit Simulation	39
Fig.4.20:	Two stage peak detector output waveform	39
Fig.4.21:	Saturation at different comparator region	40
Fig.4.22:	Simulation Model Comparator 1 and Comparator 2	41
Fig.4.23:	Two stage comparator	41
Fig.4.24:	Echo and Comparator Output	41
Fig.4.25:	Servo mounted with presumed design of sensors in front (Designed in SolidWorks).	43
Fig.4.26:	1-DOF of the Mechanical Module	43
Fig.4.27:	Test case and Software Output (Test case)	44
Fig.5.01:	Complete Module Circuitry	45
Fig.5.02:	Transmission and Echo	45
Fig.5.03:	Test case and Software Output (Field test)	46

## List of Tables

Table no.	Title	Page no.
5.01.	Tabulation for Voltage level and corresponding Distances	45
7.01.	Tabulation for Cost Estimation	48



# Contents

Title	Page no.
1 Introduction	
1.1.Motivation	12
1.2.Problem Statement	14
1.3.Objective of Research	14
1.4.Outline of the Thesis	14
2 Literature Overview	
2.1.Sonar Transducer	15
2.1.1.Radiation Patterns of Transducers and Ultrasonic Sensors	16
2.1.2.Reasons Sonar is used for Underwater Application	17
2.1.3.Equivalent Circuit Model to characterize Sonar Transducer	17
2.2.Sonar Equation	18
2.2.1.Sonar Altimeter	18
2.2.2.Transducer Parameters	19
2.3.Overview of Existing Technologies	20
2.3.1.Acoustic Bathymetry	20
2.3.2.AUVs	20
3 Transducer Parameter Evaluation	
3.1.Transducer Beam Width	22
3.2.Characteristics of Impedance	22
3.3.Transducer Power	23
3.4.Calculations for TD0200ka	23
3.5.Resonant Frequency	24
3.6.Anti-resonant Frequency	24

Title	Page no.
3.7.Co-efficient of Electromechanical Coupling	24
3.8.Mechanical	24
4 Methodology	
4.1.Generic Block Diagram	26
4.2.Electrical and Electronic Components and Module Design	26
4.2.1.Transmitter Stages	26
4.2.1.1.Ultrasonic Transducer Driving Circuit	26
4.2.1.2.Power Voltage Drive	28
4.2.1.3.Impedance Matching Network	29
4.2.2.Receiver Stage	34
4.2.2.1.Band-Pass Filter Circuit	34
4.2.2.2.Echo Detector Circuit	38
4.2.2.3.Comparator (ADC)	41
4.3.Proposed Mechanical Module Design	43
4.3.1.Linkage	43
4.3.2.Proposition of Mechanical Module:	44
4.4.Algorithm Design	45
4.5.Software Calibration	45
5 Experimentation and Result Analysis	
5.1.Lab Testing	46
5.2.Field Testing	47
5.3.Analysis	48
6 Conclusion	
6.1.Further Development	49
7 Project Management	
7.1.Project Management	50

Title	Page no.
7.2.Project Schedule	50
7.3.Cost Estimation	50
References	51
Appendix A: Components Used	55
Appendix B: Transducer Datasheet	55
Appendix C: Signal Flow Diagram	56
Appendix D: Gantt chart	57
Appendix E: Codes	58
Appendix F: Flowcharts	75

## Chapter 1

### Introduction

“The world is not an arbitrary arrangement of points floating aimlessly in Euclidean space. Environments are structured, be it by natural or human forces; they contain repetitive patterns and geometric regularities. The perceptive circuits of the human brain handle this unconsciously” [11].

But not all environments are human friendly or easily perceivable. Then, Computer perception made significant progress since Larry Robert’s Ph.D. dissertation in 1963 which laid the foundations of the field of computer vision [10].

Computer perception has made significant progress up to this point, considering its comparative naiveté. Elimination of all but the minimum assumptions is mathematically and philosophically appealing, but may not represent the best adaptation to real world conditions. Particularly in underwater world which is undoubtedly a very difficult and challenging environment and investigating there requires huge efforts from both technological and data-processing points of view. The inherently partially structured environment and difficulties caused by the nature of the propagating medium have limited the types of sensors to be used to acquire data, thus restricted knowledge of the submerged world [11]. Infrastructures have been installed manifold till now for scientific purposes, navigation and even defense application but these are time consuming, expensive and we should not forget that the underwater environment is constantly changing.

Besides, large area mapping at high resolution underwater continues to be constrained by the mismatch between available navigation compared to sensor accuracy. Nevertheless, river bed mapping is important to understand the underwater environment [12]. Accurate underwater data can also help in the planning of river widening or even making secondary channels [13]. Though real time mapping may not be completely possible with low cost equipment but the best of it may be pulled out.

The thesis has been conducted keeping in mind the affordability and accuracy of data. It has been kept in mind to enable safety, security and knowledge during navigation.

#### 1.1.Motivation:

“Bangladesh is a low-lying, riverine, South-Asian country where rivers criss - cross each other like cobwebs. It is a broad deltaic plain subject to frequent flooding and there is a small hilly region crossed by swiftly flowing rivers” [3].

Though, at present, a lot of bridges are being built to enhance communication, water-way is still a big part for communication in this country. There are a lot of places where ferry is used for communication. Bangladesh has an extensive network of waterways. In the wide-spread network 6,000 km are navigable during monsoon and 3,900 km during dry periods according to Charles Kunaka, Senior Trade Specialist, Global Product Specialist, Bangladesh Regional Waterway Transport Project [1]. He also includes that “Waterways carry one-quarter of all passenger traffic.”

In the report it is mentioned that reduced navigability is during the dry season when Least Available Depth (LAD) is only 150 days per year and the persisting problem is due of “Lack of navigational aids” as he mentions. He further added that “there is a shortage of appropriate and modern vessels” and that there can be “Provision of equipment (survey, simulators, radar, communications, etc.) and integrated logistics solutions for users”.

In the 2009 Bangladesh Transport Policy Note of World Bank, it was mentioned that high degree of penetration of the Inland Water Transport (IWT) network provides access to about 25% of the rural household in Bangladesh. [2] IWT is such a mode of transport that has been characterized as the least-cost, environment friendly, less accident-prone and low maintenance cost. We only do not see enough of the resources we can use to improve the mode of communication. Due to lack of proper technology and resource directory, we are suffering manifold in this sector. People are suffering and sometimes even dying.

According to Department of Shipping (DOS) “43% of accidents are due to human error during navigation (Data source: Adapted from Ali, 2006)”, in the World Maritime University Dissertations (2006), it was boldly mentioned “Questions to be answered are on the level of use of technology”. This doesn’t end here. Incidents occur throughout the year as daily’s present,

A news portal banglanews24 writes, “Country’s one of the most important river route Daulotdia-Paturia’s ferry services were disrupted navigation crisis and technical problem eight ferries declared stopped and two others stuck on submerged riverbed. Bangladesh Inland Water Transport Authority (BIWTA) Paturia Ghat Manager Bidyut Kumar Saha confirmed, “Meanwhile, some buses and trucks were stuck on the both sides of the ferry Ghat.”” [4],

News portal newagebd mentioned, “Dense fog disrupted ferry service on the Shimulia-Kawrakandi route on river Padma for seven hours...At least 12 ferries with 200 vehicles including buses carrying over 2,000 passengers got stranded at different points at midstream of the river...they suspended the ferry service at about 1am as marking points and buoys of mid-river became invisible due to thick fog...Several hundred vehicles including buses and goods-laden trucks got struck on the long queue on both sides of the river with suspension of the ferry service for seven hours.” [5],

Further in another article they mention, “Ferry services from major rivers ports were hampered on Wednesday because of dense fog as the on-going cold spell disrupted life” [6],

Again, in another article, “More than 500 vehicles, mostly goods-laden trucks, got struck at Shimulia Ghat in Munshiganj and Kawrakandi Ghat in Madaripur as ferry service on the route remained suspended on Sunday because of poor navigability.” [7],

Another news portal dhakatribune stated, “tug boats recovered two ferries, Shahjalal and Hamidur Rahman, after they were caught in hidden shoals at the river channel.” [8],

Found in wikipedia, the news appeared as, “ferry accident occurred on 4 December, 2009...passenger ferry collided head-on with a launch. At least 47 people were killed. The accident occurred in the morning when the river was covered by fog. Chief government official in Kishorganj district blamed the poor conditions caused by the early morning fog.” [9],

These situations and occurrences point out the crying need to develop a system to help the navigability problem. The natural causes have to be dealt with and a system has to be developed navigate when visual is compromised but the route and vehicles can still function.

### **1.2.Problem Statement:**

In Bangladesh, ferry is an important part of communication and is still irreplaceable. The problems mentioned above are mostly due to poor navigable conditions. Sometimes there is fog, sometimes there is underwater low depth riverbeds that couldn't be detected to naked eyes etc. that not only made people suffer immensely in terms of time and patience but also took lives. Under such circumstances, we have made efforts to solve the navigability by introducing a system for vehicles to monitor underwater by creating 3D real time map of the underwater surface using ultrasonic transducers to perceive the underlying environment and hereby improve the navigability on the water when visual is poor or compromised.

### **1.3.Objective of Research:**

- i) To design a system to perceive the underwater environment.
- ii) To design a software that would create a 3D map of the underwater environment in real time.
- iii) To design the system at the minimum possible cost for general affordability.

### **1.4.Outline of the Thesis:**

The first chapter explains the problem statement and the objectives to be fulfilled. The second emphasizes on the literature and available technology. The third chapter has been reserved for the transducer parameter evaluations. The fourth consists of the methodology of the proposed electrical and mechanical design followed by the algorithm and the program calibration. The rest of the chapters include experimentation, testing and the management details.

## Chapter 2

### Literature Overview

#### 2.1.Sonar Transducer:

Transducers have been used by many until now. Though it is a common device, we would like to include a small introduction to the device in order to familiarize the non-technical persons going through the paper. It is a device which can convert electrical energy into acoustic energy and vice versa. There are mainly three types of transducer piezoelectric, electrostrictive and magnetostrictive. Since materials exhibiting effect for example, quartz and Rochelle-salt started to be most commonly used, made it a prime source to construct sonar transducer. We have chosen PZT-4 material transducer, as it provides high power acoustic radiation [21]. It is mainly attained due to its high resistance of depolarization and minimal dielectric loss. Added to this, td0200ka have parallel resistance of 500 ohm in air which made it a better choice as a high power acoustic transducer. Piezoelectric transducer basically works by applying electric-field to crystals which responds by changing dimensions. Alternating field causes PZT-4 crystal to vibrate at 200 kHz within 4 kHz deviation from its source frequency range ( $f_s$ ). So, a driving frequency of 200 kHz will cause the transducer to vibrate at resonant frequency.

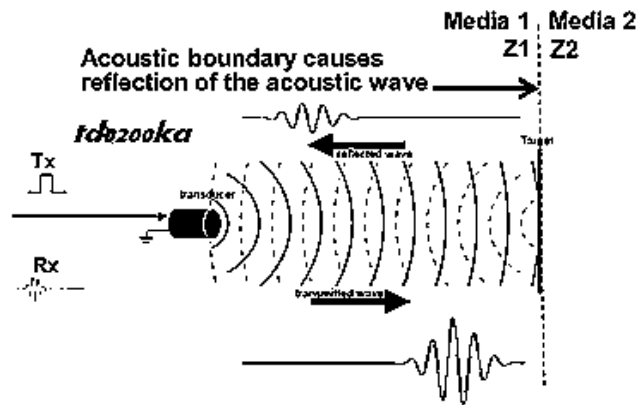


Fig 2.01: Acoustic boundary reflection in different medium Z1 & Z2 [36]

All piezo transducer has a resonant frequency that is function of material composition and mechanical dimensions. Driving at resonant frequency causes greatest amount of acoustic energy to be radiated during transmission and have greatest sensitivity. Return echo is guided by an acoustic boundary, where difference in medium Z1 and Z2 reflects echo, signal strength gets lower than what it was transmitted. Reflected echo will be maximum, if the speed of sound between the barriers are furthest separated, that is,  $n = Z1 \sim Z2$  is maximum. At acoustic boundary some energy passes through and some reflects depending on reflection and transmission coefficient exhibiting at the barrier. Reflected wave is our desired echo signal. Transducer later detects echo and turns into electric signal.

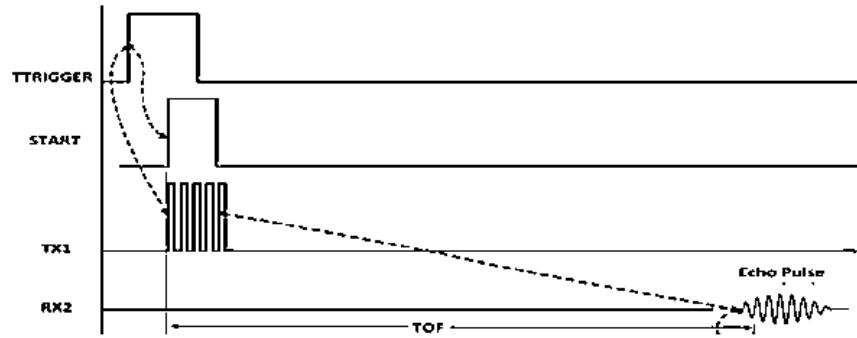


Fig 2.02: Transmitted and echo pulse [37]

Trigger from MCU starts the process, where transducer transmits ultrasonic pulse of 200 kHz. Ultrasonic is any sound ranging above audible frequency 20 kHz. Most of the sonar used for underwater application are within 30 kHz – 5 GHz range [22]. After receiving echo pulse distance or under water depth (required for our purpose) is calculated by 'time of flight' equation.

$$D \text{ (depth)} = \frac{TOF * C_{\text{medium}}}{2}$$

Since, we are more interested in sonar mapping (of river bed), we require collection of these echo pulses. Sonar range can however be limited by the major two losses:

- i) Beam-spreading loss
- ii) Acoustic absorption

### 2.1.1. Radiation Patterns of Transducers and Ultrasonic Sensors:

The acoustic radiation pattern, or beam pattern, is the relative sensitivity of a transducer as a function of spatial angle. This pattern is determined by factors such as the

- i) Frequency of Operation, FOP
- ii) Size, shape, and acoustic phase characteristics of the vibrating surface.

The beam patterns of transducers are reciprocal, which means that the beam will be the same whether the transducer is used as a transmitter or as a receiver. It is important to note that the system beam pattern of an ultrasonic sensor is not the same as the beam pattern of its transducer. Transducers can be designed to radiate sound in many different types of pattern, from omnidirectional to very narrow beams. For a transducer with a circular radiating surface vibrating in phase, as is most commonly used in ultrasonic application, the narrowness of the beam pattern is a function of the ratio of the diameter of the radiating surface to the wavelength of sound at the operating frequency. The larger the diameter of the transducer as compared to a wavelength of sound, the narrower the sound beam. Narrower beam provides greater directivity so a beam width of 14° would provide an optimum result keeping balance in signal power strength (directivity) and sonar cone coverage. Illustration have been made below to show estimation of coverage can be obtained. The equation has been cited [39].



$$D(\text{Sonar Angular Cone Diameter}) = 2 * \text{depth} * \tan\left(\frac{\angle \text{cone angle}}{2}\right)$$

Parameters from td0200ka datasheet, cone angle  $\theta = 14^\circ$ , suppose we want to map for a maximum depth of 50m. Then maximum cone diameter  $D = 2 * 100 * \tan(7^\circ) = 87.1$  m coverage which is far more than our required range [24]. Directivity pattern provides detection of object position within spectral lobe. Whenever, any object punches this lobe echo is been received. We used build in MatLab function 'polarpattern(angle, magnitude)' to generate directivity pattern as shown below.

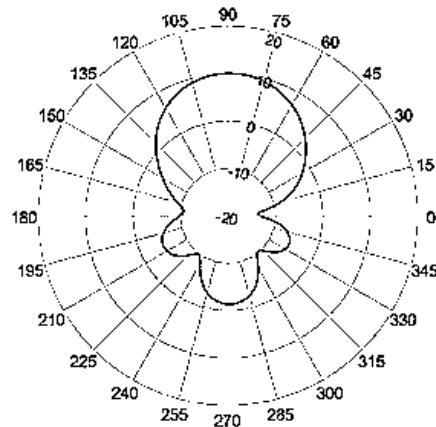


Fig 2.03: MatLab polarpattern [38]

### 2.1.2.Reasons Sonar is used for underwater application:

- Attenuation (beam) is much less in H<sub>2</sub>O than in air.
- Objects can be detected at much greater ranges using echo location in H<sub>2</sub>O rather than in air.
- Surface subjected to radiation in underwater transducer only have to move small displacements to generate larger sound pressures.

### 2.1.3.Equivalent circuit model to characterize sonar Transducer:

Mechanical and acoustical portions of transducer were modelled by converting into equivalent electric circuit components of R, L, C. Transducer can be characterize into two major parts mechanical and acoustic portion

$$\text{Transducer} = \text{Mechanical portion} + \text{Acoustic portion}$$

On acoustic portion, equivalent circuit elements were coupled to pure electrical portions of the transducer by electro-mechanical device. Heading towards designing transducer equivalent circuit we go back to basic electric principle, ohm's law. From ohm's law in an electric circuit we can deduce that current flowing across an impedance 'Z' and terminal voltage 'E' is given by

$$E = IZ$$

In acoustic sound pressure 'P' of acoustic wave is equivalent to voltage 'E' in electric circuit. So, our first analogy is  $P = E$ , unit  $\mu\text{Pa}$ . Particle velocity 'u' is analogous to current 'I'. There comes our second analogy  $u = I$ , unit m/sec. Acoustic impedance of transmission medium is the product of density ( $\rho$ ) and speed of sound in the medium(c). Hence, our final analogy follows is  $\rho * c = Z$ , unit ohms or rayls. Acoustic impedance in H<sub>2</sub>O is much greater than that in air,  $\rho_c|_{\text{H}_2\text{O}} \gg \rho_c|_{\text{air}}$ . Medium variance for sonar transducer must generate relatively large amount of force 'F' to compress high dense H<sub>2</sub>O.

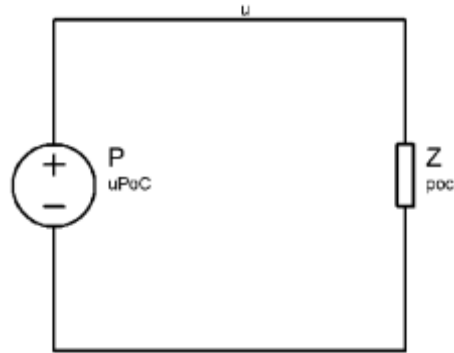


Fig 2.04: Electrical equivalent circuit of transducer [created in proteus]

## 2.2.Sonar Equation:

Sonar system separates desired signal from unwanted background noise. As depth sounder radiates 'pulse', signal spreads conically away from transducer. Results in decrease in amount of energy, known as 'spreading loss'. In addition attenuation effect or absorption losses are there on pulse.

$$\text{Transmission loss} = \text{Spreading loss} + \text{Absorption loss}$$

The amount of acoustic signal, reflected back is known as backscattering strength of target. Considering losses and modelling sonar into different equations we can derive sonar equations.

Firstly, taking signal-noise- ratio into account since we are using passive sonar equation because it is simpler and will allow us to define some terms and notation. Of fundamental importance to sonar is the signal-to-noise power ratio (SNR) achieved [40]:

$$\frac{S}{N} = \left( \frac{\text{Signal}}{\text{Prop Loss}} \right) \times \left( \frac{\text{Array Gain}}{\text{Total Noise}} \right)$$

Here 'Prop loss' is the propagation loss and 'signal' is the radiated signal power. Power loss as shown in figure 01 can be depicted by [40]:

$$\text{dB}_{\text{loss}} = 10 \log_{10} [4 * Z_1 * Z_2 * (Z_1 + Z_2)^2]$$

### 2.2.1.Sonar Altimeter:

As we have seen earlier an electrical signal is sent to transducer that transmits acoustic signal into water. Same transducer stops transmitting to receive an echo signal. We need to take echo having

greatest signal value less attenuated by noise. Echo requiring least TOF (time of flight) is the signal having greatest strength. In our Processing code while receiving multiple echo (echo 1, echo2, echo 3....), echo having maximum signal power have been taken to calculate our required distance 'd' .

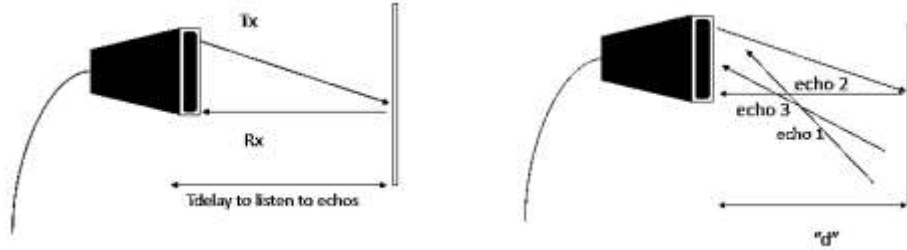


Fig 2.05: Distance from multiple echo calculation [created in MS Powerpoint]

### 2.2.2. Transducer Parameters:

i) **Sensitivity:** Td0200ka have receive sensitivity of -190dB, which is quite expected for pzt-4 materials. Due to its high sensitivity we can attain wider BW (band width - kHz). Large mismatch in impedance reduces material sensitivity. It is defined as an ability of transducer to detect small defects in transducer [25].

$$\text{Sensitivity} \propto \text{BW};$$

$$\text{Sensitivity} \propto \frac{1}{Z_{\text{mismatch}}}$$

ii) **Penetration:** Measure of directivity, penetration property increases with power.

$$\text{Penetration} \propto Z_{\text{mismatch}}$$

iii) **Resolution:** It is the ability to separate signals produce by two reflectors when close to each other.

$$\text{Resolution} \propto \text{Damped(dampness)}$$

iv) **Central frequency ( $f_r - 200$  kHz):** It depends backing of materials. Highly damped transducers, will respond to frequency (above and below of central frequency). Greater ' $f_r$ ' provides reduced penetration but high sensitivity.

$$f_r \propto \text{Sensitivity};$$

$$f_r \propto \frac{1}{\text{Penetration}}$$

v) **Frequency Range (4 kHz):** Broad frequency range provides transducer with high resolving power.

$$f_{\text{range}} \propto P_{\text{resolving}}$$

**vi) Damped transducer:** Highly damped transducer helps to shorten the reflected pulse to provide high resolution. In contrary, less damped transducer allows narrower frequency range and poor resolving power but with greater penetration power. So, if we want achieve high resolution we have to trade off 'penetration power.'

## **2.3.Overview of Existing Technologies:**

### **2.3.1.Acoustic Bathymetry:**

Sound wave have always been preferred over electromagnetic wave in bathymetry owing to the fact that sound wave propagates longer distances. As we wave through history, both shallow and deep water acoustics studies were pursued extensively during Second World War. The discovery of Ewing and Worzel marked the beginning of bathymetry [14]. Other than sonar, there are four commonly used techniques for riverbed topography by the mean of remote sensing [15], which are:

**a. Spectral methods utilizing correlation between depth and light absorption**

**b. Ground penetrating radar (GPR)**

**c. Bathymetric LIDAR (Light Detection And Ranging)**

**d. Photogrammetry**

However we emphasize on echo sounding technique which measures water depth through the transmission and echo detection of acoustic pulse. Until early 1960s, single-beam sonar were considered as the primary instrument of depth sounding. After revolution with invention of expansive multi-beam sonar, high resolution echo reflective map can be produced with much less time [16]. Wide-beam transducers detect echo with a large angle under vessels and is useful for safe navigation routing whereas narrow-beam sounder are capable of providing high spatial resolution with small angle but are incapable of covering large area with each ping [16]. Even with single-beam sonar where incident angle nears zero, it improve reproducibility and reliability of acoustic waterbed classification [17]. Further down the line, biomimetic sonar systems, using wide beam and wide bands could also be used in localizing and classifying as presented by Qiang Wang in his paper [18].

Sonar used in bathymetry are active sonar and return echo which are then analyzed to define shapes using different techniques for mapping the underwater environments.

### **2.3.2.AUVs:**

Many Automated Underwater Vehicles (AUV) have been built for underwater perception. They map waterbeds to understand the underwater environment better. We came across many of the AUVs that have been designed so far. Some were even autonomous and had their own algorithms for perception. Most of them had sonar in common though, the data received were manipulated

and structured in different procedures to perform the task at hand. We came across many different approaches.

Among them a few mention worthy methodologies are Structure from motion (SfM) used by Klaus and Gabriele where they estimated 3D structures from 2D image sequences coupled with local motion signals [19], students from Santa Clara University developed a SWATH boat for shallow-water bathymetry. In that project, they used a Imagenex Multi-beam Sonar along with Teledyne Instruments Workhorse Doppler Velocity Log (DVL) and Garmin 18 differential GPS receiver to create bathymetric maps [20], Zhong, C. H. obtained depth sensor data, passed into Peaks function in MatLab, demonstrated mesh graph and 3-D shaded surface, directed to Surf function and applied it to form 3-D shaded surface to generate the 3D graph [12] etc. All the above examples required to acquire all the data beforehand to create the map of the water surface.

After a thorough overview of the literature ahead of us, we devised plans to work on our own design and algorithm to create a system capable of real time 3D mapping of the environment.

## Chapter 3

### Transducer Parameter Evaluation

#### 3.1. Transducer Beam width:

Transducer beam angle determines horizontal beam width at corresponding depth levels. If the beam angle is more our target area coverage in identifying targets will also be more. But, the tradeoff is penetration and signal intensity reduces. Narrower beam width is more intense and have greater likelihood in reaching deeper depths. In measuring transducer's cone angle power is initially calculated at the center axis which is commonly known as the 'beam axis'(as shown in figure). This power is compared to half power point (-3dB) either side of the axis. Subtended arc between half power points is the beam or cone angle ' $\alpha$ '.

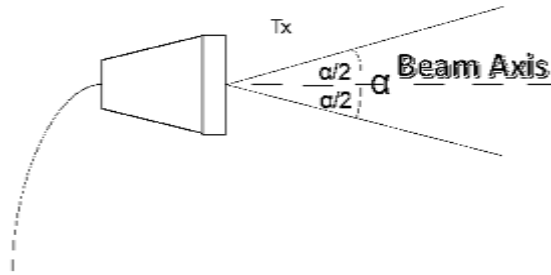


Fig.3.01: Beam angle definition [created in MS Powerpoint]

Beam angle width can be expressed as [41],

$$\sin\left(\frac{\alpha}{2}\right) = 0.514 * \frac{c}{f * d}$$

c – speed of sound in medium tested  
f – frequency of transducer beam  
d – Element Diameter

Our beam angle is approximately  $14.1^\circ$ , which means it can detect object within this vicinity. At, constant power narrow beam cone will produce same amount of power but in small region, compared to wide beam cone.

#### 3.2. Characteristics of Impedance:

Impedance of transducer coaxial cable is of interest to find out how much power is drawn across the wire. It can easily found by calculating ratio of inner diameter of outer conductor 'D' to outer diameter of inner conductor 'd'. Since, material medium plays a big role in cable impedance value of ' $\epsilon$ ' in environment tested needs to be known [42].

$$\text{Impedance } Z_0 = \frac{138}{\epsilon} * \log\left(\frac{D}{d}\right)$$

Where, D and d are outer and inner conductor diameters respectively.

Per unit length characteristics equation can be simplified to electrical parameters of coaxial cable.

$$Z_0 = \sqrt{\frac{L}{C}}$$

In our transducer module, during transmission 555 timer which excites the piezo ultrasonic transducer is the source and the transducer itself is the load. On detection, transducer becomes the source and echo detector circuit in receiver side is the load.

### 3.3. Transducer Power:

Piezo-electric transducer exerts constant power in transmitting a signal. Narrow beam transducer will have greater directivity (intensity) and be more powerful. Greater output power yields deeper range. Moreover, it ensures stronger echo return. High power transmitted signal increases the likelihood of getting an echo from deep water with greater depth. It also provides high resolution, separates mapped image into more pixels giving better illustrations.

Ability of sonar to differentiate between targets referred to as range resolution. Range resolution can be calculated as,

$$R(\text{range resolution}) = \frac{1}{2} (\text{pulse length} * \text{velocity of sound in water})$$

### Comparison between 200 kHz & lower frequency transducer:

200 kHz transducer have:

- i) Have shallower depths
- ii) Narrow cone angle
- iii) Better definition and target separation
- iv) less noise susceptibility
- v) provides better resolution and definition of structure and object
- vi) Can show small object under water

### 3.4. Calculations for TD0200ka [Appendix E, Block: 4]:

**L<sub>1</sub> (series inductance) = 13.236637mH**

**R<sub>1</sub> (series Resistance) = 353.384430Ω**

**F<sub>p</sub> (parallel resonance) = 204 kHz**

**C<sub>o</sub> (Parallel capacitance) = 3.204421nF**

**f<sub>1</sub> = 199.0315 kHz**

**C<sub>1</sub> (series capacitance) = 0.047358nF**

**F<sub>s</sub> (series Resonance) = 201.024 kHz**

**C<sub>T</sub> (transistor capacitance) = 3.251779nF**

**C (static capacitance) = 1500pF**

**f<sub>2</sub> = 203.2805 kHz**

### 3.5. Resonant frequency, $f_r$ :

An input excitation sinusoid voltage applied to a transducer. Whenever the input voltage matches natural frequency of transducer, vibration becomes rapid. This frequency is known as resonant frequency. These equations have been cited [43].

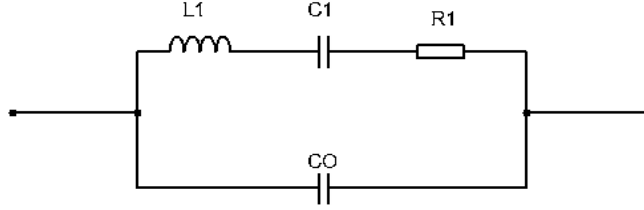


Fig.3.02: Transducer equivalent circuit (same as Butterworth impedance matching model)

$$f_r = \frac{1}{2\pi\sqrt{L_1 C_1}}$$

$$f_r = 201.0179 \text{ kHz}$$

### 3.6. Anti-resonant frequency, $f_a$ :

In impedance characteristics graph, frequency at which transducer impedance reaches its peak value is the anti-resonant frequency.

$$f_a = \frac{1}{2\pi * \sqrt{\frac{L_1 * C_0 * C_1}{C_1 + C_0}}}$$

$$f_a = 202.498 \text{ kHz};$$

### 3.7. Co-efficient of electromechanical coupling:

It represents the mechanical energy accumulated in pzt-4 which depends on total electrical input. This parameter can be calculated for each vibration mode using resonant frequency ( $f_r$ ) and anti-resonant frequency ( $f_a$ ).

$$k_r = \sqrt{\frac{1}{0.395 * \left(\frac{f_r}{f_a - f_r}\right) + 0.564}}$$

$$k_r = 0.1802$$

### 3.8. Mechanical, Q :

It measures sharpness of mechanical vibration at resonant frequency.



$$Q_m = \frac{f_a^2}{2\pi f_r Z_r C (f_a^2 - f_r^2)}$$

Where,  $Z_r$  is the series resistance

Another, simpler equation which is in terms of 3dB frequency components  $f_1$  &  $f_2$ .

$$Q_m = \frac{f_r}{|f_1 - f_2|}$$

$$Q_m = 47.308$$

We can find resonant resistance, by substituting  $Q_m$  value

$$Z_r = \frac{f_a^2}{2\pi f_r Q_m C (f_a^2 - f_r^2)}$$

$$Z_r = 766.04 \Omega$$

## Chapter 4

### Methodology

#### 4.1. Generic Block Diagram:

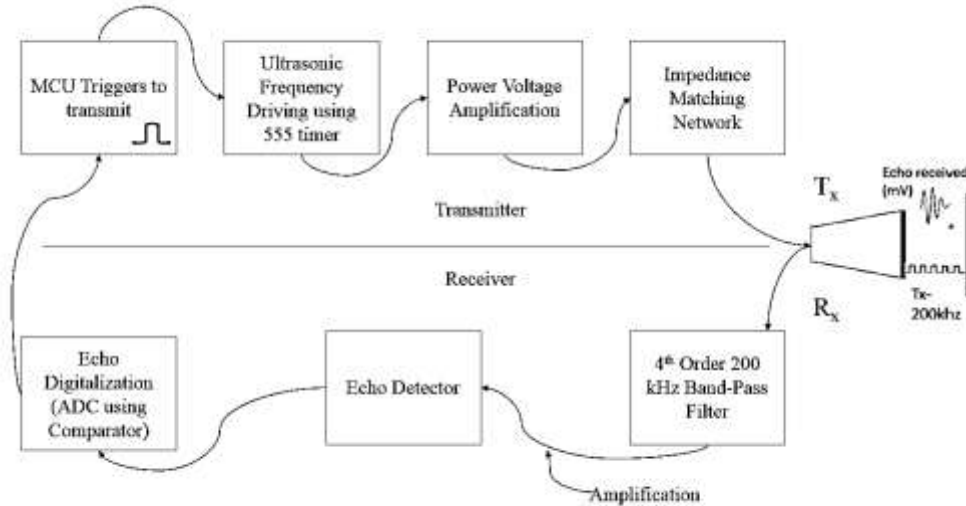


Fig 4.01: Block Diagram of Ultrasonic Transducer Communication System [created in MS Powerpoint]

#### 4.2. Electrical and Electronic Components and Module Design:

The electrical and electronic module designs consists of the transmitting and receiving stages. The primary triggered signal from the MCU is processed through the designed circuit stages for transmitting and after an echo is pinged, the echo signal is delivered to the MCU via filtering and refining.

##### 4.2.1. Transmitter Stages:

The transmitter stages consists of triggering pulse excitation from the MCU followed by the generation of transducer required frequency pulse using Ultrasonic Transducer Driving circuit. This pulse is then amplified and impedance matched using Power Drive and impedance Matching circuit to transmit the transducer rated power equivalent signal.

##### 4.2.1.1. Ultrasonic Transducer Driving Circuit:

In this stage, the MCU generates the triggering signal which in turns activates the 555 chip via a bipolar junction transistor. This BJT acts as a switch to regulate the generation and transmission of signal for the transducer. When triggered through arduino,  $V_{cc}$  is supplied to the chip and hereby starts generating the 200 kHz signal for transmission. The 555 timer has been configured to generate 200 kHz frequency by setting up a value for the capacitor and then calculating the ratio of the resistors accordingly.



## Oscilloscope Waveforms:

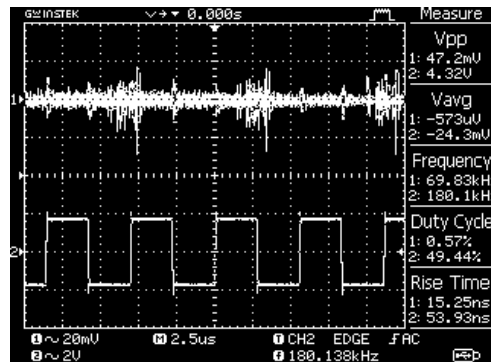


Fig 4.04: Oscilloscope View of 200 kHz generation and arduino triggering

As it is seen from fig. 3.01, the triggering signal from the Arduino board pin 7 activates the 555 timer chip  $V_{cc}$  and hereby start generation. When the trigger stops, the  $V_{cc}$  turns LOW and hereby the reset pin of 555 shorted to  $V_{cc}$  activates and resets the oscillation. This bizarre setup has been made owing to the fact that arduino trigger high only generates a 1 kHz pulse and not a 200 kHz pulse as required for the selected transducer.

### 4.2.1.2. Power Voltage Drive:

The power voltage drive is very important in terms of transducer activation. As the transducer we used is rated at 20W, the signal must be 200V p-p. The 555 timer circuit used in the oscillatory circuit is biased at 10V, the signal follows the voltage. We needed to boost the voltage to 200V. Primarily we tried to use a transformer and then also tried the boost converter module to increase the voltage. This created a problem as very high frequency signal generation causes very high power loss in the inductor coils. Most transducer systems today use toroid transformers, which was unavailable to us. Thus we decided to boost the voltage using a regular amplification circuit. The voltage was amplified using an operational amplifier setting in non-inverting conditions where we required 8 stages of amplification in practical to convert the starting voltage to almost 200V p-p. The signal was now almost proper 200 kHz 200V p-p as required for transmitting through the transmitter. The equation is the generic non-inverting amplifier configuration equation.

### Simulated Circuit:

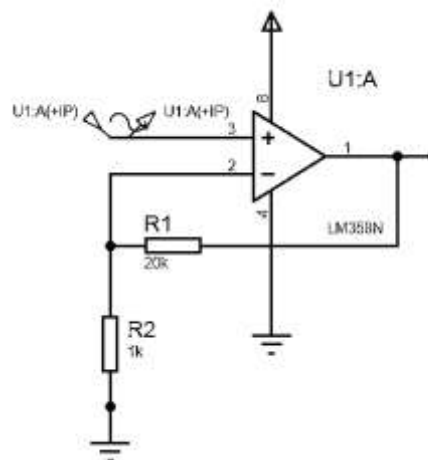


Fig.4.05: Power Voltage Drive [created in proteus]

### Circuitry:

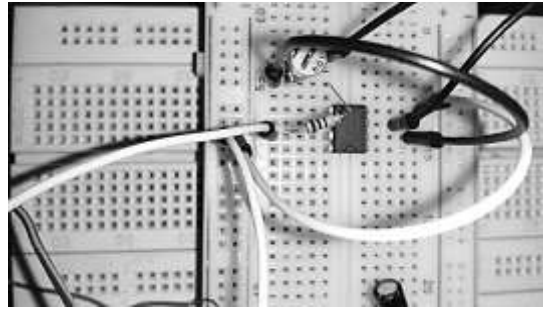


Fig.4.06: Single Stage Amplification

### Calculation:

$$A_v = \frac{V_{out}}{V_{in}} = 1 + \frac{R_1}{R_2}$$

$$R_1 = 20k\Omega$$

$$R_2 = 1k\Omega$$

$$A_v = 21$$

#### 4.2.1.3. Impedance Matching Network:

We require optimum impedance matching circuit in order to ensure that maximum energy is transmitted for strongest echo. Considering, piezo transducer as reactive load which can be represented by 'R<sub>s</sub>' (series resistor) and 'C' (capacitor) which depends on frequency. For simplicity in our calculation, we made parallel equivalent of series circuit.

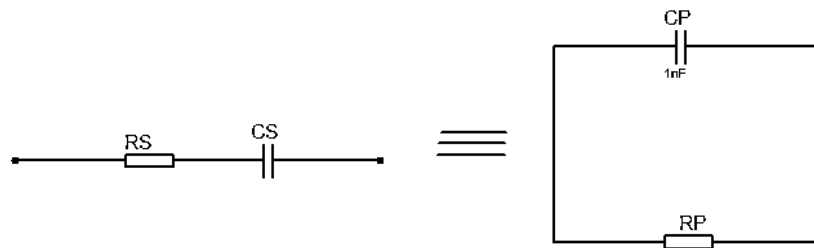


Fig.4.07: Parallel Equivalent Circuit for modelling

The main goal is to obtain best echo, for that we need to design R<sub>eq</sub> and C<sub>eq</sub> in such a way that circuit works at resonance frequency (f<sub>r</sub>). We know from maximum power theorem that, when source resistance equals load resistance than maximum power is transferred to load.

$$P_{max} = \frac{1}{2} \frac{V_p^2}{R}$$

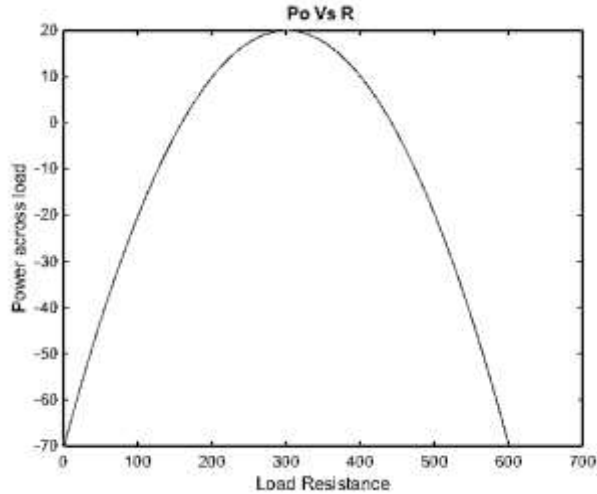


Fig.4.08: Maximum Power Transfer [Appendix E, Block: 5]

Effectiveness may be ensured by placing equivalent parallel capacitance,  $C_p$ , of Piezo device across inductor (L).  $R_{eq}$  across inductor required to calculate power dissipation. Peak power should occur at the value of parallel resistance,  $R_p$ , if it does not occur adjustment has to be made in turns ratio 'a' and Quality factor, Q. We would initially calculate transducer parameters than show few assumption based on what alteration is been made [29].

**Method I: Series equivalent values of Piezo device**

Inductor which is in series with piezo device, have reactance chosen to be equal to reactance of series equivalent capacitance,  $X_c$  [ $X_L = X_C$ ].

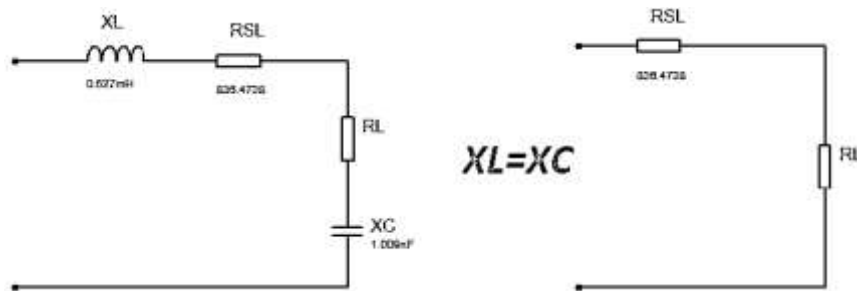


Fig.4.09: Series Resonance equivalent circuit

We know,

$$f'_{res} = \frac{1}{2\pi\sqrt{LC}}$$

In resonance frequency the value of L and C are of our interest. From, td0200ka (datasheet) Parallel resistance

$R_p = 500\Omega \pm 30\%$ ,  $P_{rated} = 20W$ ;  $f = 200 \text{ kHz}$ ;  $C \text{ (static)} = 1500\text{pF}$ .

$$R_p = \frac{(R_s + X_{CS}^2)}{R_{SL}}$$

$$X_c = \frac{1}{2\pi f C}$$

$$X_c = \frac{1}{2\pi * 200k * 1500p}$$

$$X_c = -j530.52\Omega$$

From, equation  $R_p$ ,  
 $R_{SL} = 836.47\Omega$ .

Parallel reactance

$$X_{CP} = \frac{R_{SL} * R_P}{X_c}$$

Substituting the value of  $R_{SL}$ ,  $R_p$  and  $X_c$

$$X_{CP} = 788.4\Omega$$

$$X_{CP} = \frac{1}{2\pi f C_p}$$

$$C_p = 1.009nF$$

At resonance frequency  $f_{res}$  ' $X_{LP} = X_{CP}$ ', hence we can find inductor value

$$L = \frac{X_{CP}}{2\pi f}$$

$$L = 0.627mH$$

Quantity factor, Q

$$Q = \frac{R_p}{X_{LP}}$$

$$Q = 1.06$$

Since, 'Q' here is only 1.06 we want better quality factor to match what it is likely be more reactance value 'X'.

Let us assume for quality factor '8' which is sufficient for our case.

$$X = \frac{R_p}{Q}; [X = X_L = X_C]$$

$$X = 104.56\Omega$$

Again,

$$L = \frac{X_L}{2\pi f}$$

$$L = 83.2\mu H$$

As expected we need to add more capacitance value to match reactance above.

$$C' = \frac{1}{2\pi f X_L}$$

$$C = 7.61nF$$

Amount of capacitance needed to be added:

$$C' - C = 7.61\text{nF} - 1.009\text{nF}$$

$$\Delta C = 6.601\text{nF}$$

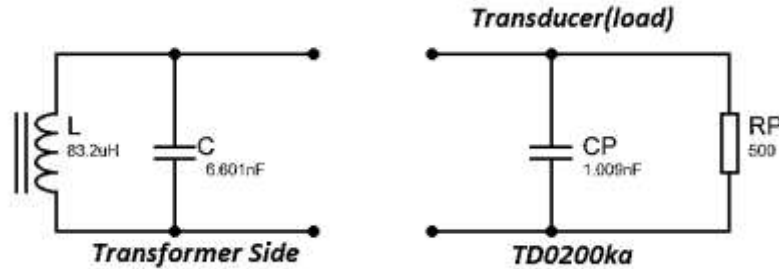


Fig.4.10: L, C Value to match Transducer Impedance

We, need to be precise in choosing which transformer to use. Coupling factor 'k' should be as close to 1 as possible, following there is little flux leakage from the transformer [30]. Best coupling is obtained as primary coil is wound tightly over the secondary.

### Power into Piezo Device:

Maximum power that can be transmitted to transducer should not exceed the rated value.

$$P_{\text{transferred}} \leq P_{\text{rated}}$$

Power equation, can be solved for maximum voltage and current value. Using basic circuit power equation, we know,

$$P = \frac{E_{\text{rms}}^2}{R_p}$$

$$E_{\text{rms}} = \frac{E_{\text{peak}}}{\sqrt{2}}$$

$$P = \frac{E_{\text{peak}}^2}{2R_p}$$

$$P_{\text{rated}} = 20\text{W (td0200ka)},$$

$$E_{\text{peak}} = \sqrt{20 * 2 * 500}$$

$$E_{\text{peak(max)}} = 141.42\text{V}$$

$$E_{\text{rms}} = 100\text{V}$$

It can be deduced that maximum current that can flow at Maximum Voltage  $E_{\text{peak}}$  is,

$$I_p(\text{max}) = \frac{P}{E_{\text{peak}}}$$

$$I_p = 0.2\text{A}$$



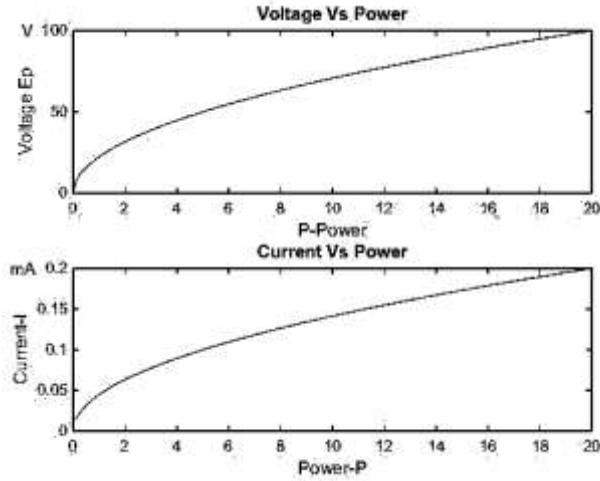


Fig.4.11: Power Vs Current/ Voltage Characteristics [Appendix E, Block: 6]

## Method II: Butter-worth Van Dyke Ultrasonic Transducer Model

The Butterworth Van Dyke model suggests that the transducer be modelled as a resistor and a capacitor in parallel [28]. All equations have been taken from the mentioned reference [28].

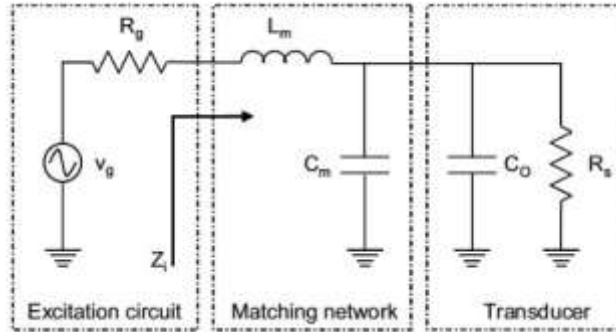


Fig.4.12: Impedance Matching [28]

$Z_s$  is the load seen by source and the transfer function is defined as,

$$Z_s = \frac{1}{\omega C_L} \frac{(\omega_s^2 - \omega^2) + j \left( \frac{R_s}{L_s} \right) \omega}{-\left( \frac{R_s}{L_s} \right) \omega + j (\omega_p^2 - \omega^2)}$$

$$\omega_s^2 = \frac{1}{L_s C_s}$$

$$\omega_p^2 = \frac{C_s + C_L}{L_s C_s C_L}$$

$\omega_s = 1263.07 * 10^3 \text{ kHz}$  and  $\omega_p = 1281.76 * 10^3 \text{ kHz}$ , the series and parallel resonance frequencies respectively.

The  $L_m$  and  $C_m$  can be resolved by the equations:

$$L_m = \frac{R_g}{\omega} \sqrt{\frac{R_L}{R_g} - 1}$$

$$C_m = \frac{1}{\omega R_L} \sqrt{\frac{R_L}{R_g} - 1} - C_L$$

Now, using any of the above methods impedance can be matched, we used the second method.

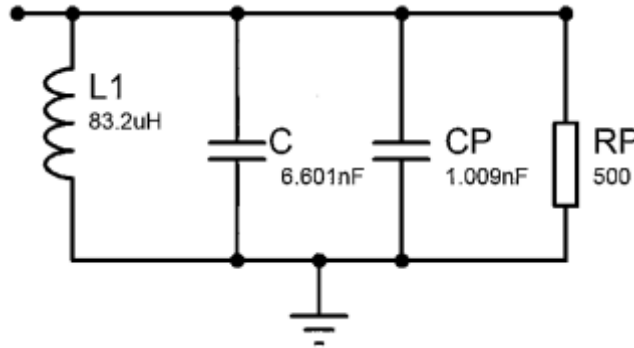


Fig.4.13: Impedance Matching Circuit [created in proteus]

Impedance needs to be matched in order to get maximum power transfer. Otherwise, there will be unnecessary power loss in the system. Moreover, the transducer needs a specific amount of power to turn on, the rated power of the transducer. The ultrasonic voltage drive circuit supplies a very small amount of voltage, about 5V at 200 kHz from the arduino. After amplification the signal becomes 200V p-p. This signal needs to be impedance matched in accordance to the maximum power transfer theorem to produce the actual trigger signal to be supplied to the ultrasonic transducer. That has been calculated and finally transmitted.

#### 4.2.2.Receiving Stage:

The receiving stages deal with the signal echoed to the transducer. The signal is band pass filtered to retain the frequency of oscillation and then peak detection is done via envelope detector circuit configuration for noise cancellation. This is then passed through the echo detector circuit to find the echoed pulse and finally sent to the MCU for processing and calculations.

##### 4.2.2.1.Band Pass Filter Circuit:

The echo received will definitely be contaminated with noise and thus requires to be filtered. Generally, the higher the order of the filter the better the reception of signal. We chose 4<sup>th</sup> order band pass filter for the process as higher order filters contain risk factor of cutting off the original signal bandwidth for even may cause attenuation of the actual echo signal to be detected by the echo detector circuit. We used the Butterworth's active band-pass filter using Multiple Feed Back (MFB) topology for 4<sup>th</sup> order band-pass filter design [26]. The filter is made up of two 2<sup>nd</sup> order filters cascaded to perform 4<sup>th</sup> order filtration. All equation have been taken from mentioned reference [26].

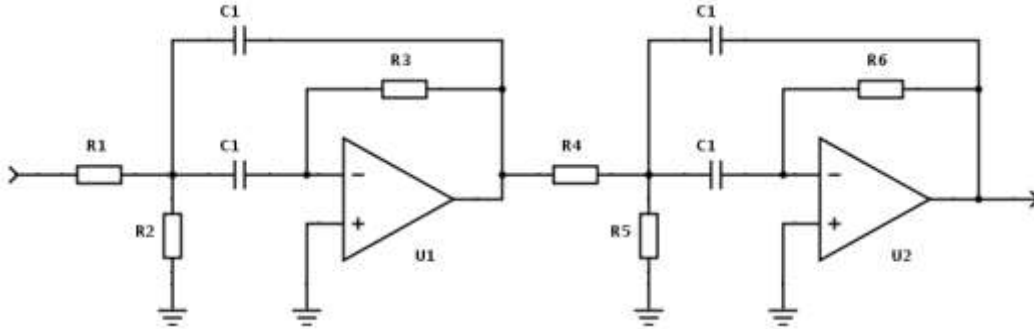


Fig 4.14: Generic Butterworth's 4<sup>th</sup> Order Active Band-pass filter using MFB topology [26]

Designing a generic 2<sup>nd</sup> order filter from transfer function using a Butterworth's 2<sup>nd</sup> order active band pass filter using MFB topology, the transfer function is,

$$A(s) = \frac{A_m \omega s}{1 + \omega s + s^2}$$

The quality factor Q is given by,

$$Q = \frac{f_m}{BW}$$

Or,

$$Q = \pi f_m R_2 C$$

The mid frequency,  $f_m$  is given by,

$$f_m = \frac{1}{2\pi C} \sqrt{\frac{R_1 + R_3}{R_1 R_2 R_3}}$$

The overall gain,  $A_m$  is given by,

$$A_m = -R_2 / 2R_1$$

The separate resistors are calculated from the equations,

$$R_1 = \frac{R_2}{-2R_1}$$

$$R_2 = \frac{Q}{\pi f_m C}$$

$$R_3 = \frac{-A_m R_1}{2Q^2 + A_m}$$

This is done so because the generic transfer function of a 4<sup>th</sup> order band-pass filter is given by

$$A(s) = \frac{\left(\frac{A_m \omega^2}{b_1}\right) s^2}{1 + \left(\frac{a_1}{b_1}\right) \omega s + \left(2 + \frac{\omega^2}{b_1}\right) s^2 + \left(\frac{a_1}{b_1}\right) \omega s^3 + s^4}$$

This transfer function can be curtailed into two 2<sup>nd</sup> order band-pass filters,

$$A(s) = \left[ \frac{\left(\frac{A_{mi}}{Q_i}\right) \alpha s}{1 + \left(\frac{\alpha s}{Q_i}\right) + (\alpha s)^2} \right] \left[ \frac{\left(\frac{A_{mi}}{Q_i}\right) \cdot \left(\frac{s}{\alpha}\right)}{1 + \left(\frac{1}{Q_i}\right) * \left(\frac{s}{\alpha}\right) + \left(\frac{s}{\alpha}\right)^2} \right]$$

Where,

$A_{mi}$  is the gain of each partial mid frequency and is the same for both the filters,

$Q_i$  is the pole quality of the partial filters and same goes for both the filters during calculation.

For calculation of  $\alpha$  and  $1/\alpha$  the underlying equation is used.

$$\alpha^2 + \left[ \frac{\alpha \cdot \omega \cdot a_1}{b_1(1 + \alpha^2)} \right]^2 + \frac{1}{\alpha^2} - \left[ \frac{\omega^2}{b_1} \right] = 0$$

The Butterworth's coefficient for 2<sup>nd</sup> order filter are  $a_1 = \sqrt{2}$  and  $b_1 = 1$ . The derived value of  $\alpha$  from the equation can be used to design the filter using

$$f_{m1} = \frac{f_m}{\alpha}$$

$$f_{m2} = \alpha f_m$$

$$Q_i = Q_{bp} \left[ \frac{(1 + \alpha^2) b_1}{\alpha \cdot a_1} \right]$$

$$Q_{bp} = \frac{f_m}{f_H - f_L}$$

$$A_{mi} = \left( \frac{Q_i}{Q_{bp}} \right) \sqrt{\frac{A_m}{b_1}}$$

$$R_{11} = \frac{R_{21}}{-2A_{mi}}$$

$$R_{21} = \frac{Q_i}{\pi f_{m1} C}$$

$$R_{31} = -\frac{A_{mi} R_{11}}{2Q_i^2 + A_{mi}}$$

$$R_{21} = \frac{R_{22}}{-2A_{mi} Q_i}$$

$$R_{22} = \frac{Q_i}{\pi f_{m2} C}$$

$$R_{32} = -\frac{A_{mi} R_{21}}{2Q_i^2 + A_{mi}}$$

Here,  $f_{m1}$  and  $f_{m2}$  are the partial mid frequencies,  
 $f_H = 204$  kHz and  $f_L = 196$  kHz are the actual cut-off frequencies,  
 $f_m = 200$  kHz is the overall mid frequency,  
 $A_m$  is the overall gain and is taken as 2,  
 $Q_{bp} = 25$  is the overall bandpass quality factor.

When the values are plugged into the equations, the system yields,

$$R_1 = 0.369 \text{ k}\Omega \quad R_4 = 0.344 \text{ k}\Omega$$

$$R_2 = 0.003 \text{ k}\Omega \quad R_5 = 0.003 \text{ k}\Omega$$

$$R_3 = 2.44 \text{ k}\Omega \quad R_6 = 2.174 \text{ k}\Omega$$

C has been taken into account on the basis of availability and thus is  $C=10\text{nF}$

### Simulated Circuit:

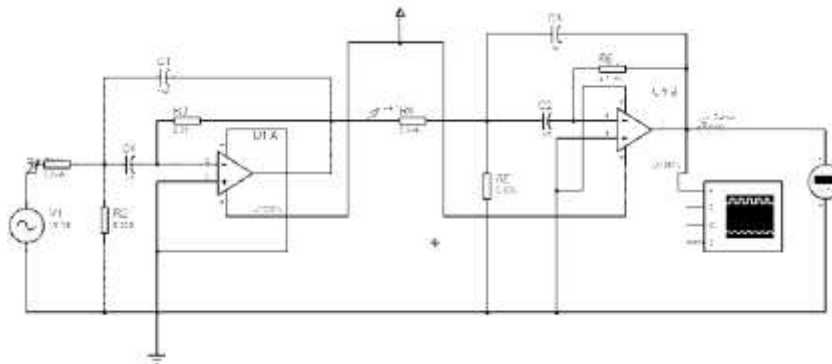


Fig.4.15: Butterworth's 4<sup>th</sup> Order Active Band-Pass filter using MFB topology [created in proteus]

### Circuitry:

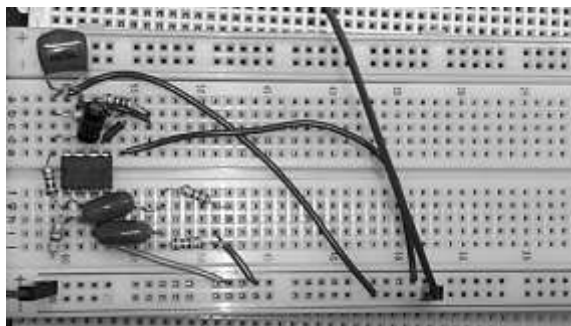


Fig.4.16: Butterworth active Band pass filter using MFB topology

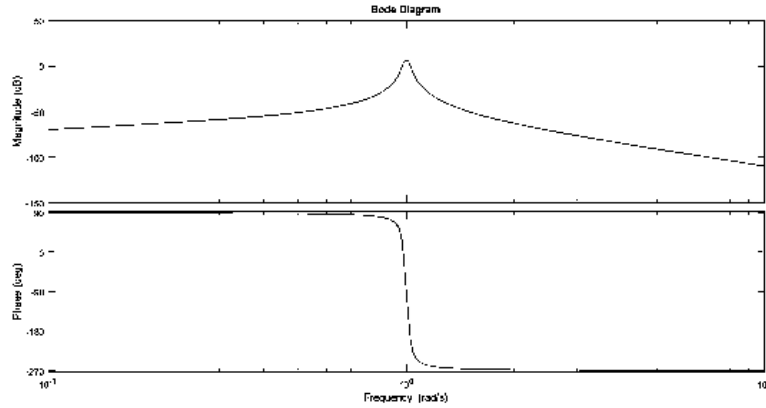


Fig.4.17: Bode Plot and Phase Diagram of designed Filter [coded in MatLab Appendix E code block]

#### 4.2.2.2. Echo Detector Circuit:

High frequency sound wave as they are transmitted gets far more attenuated than lower frequency. Intensity at which sound wave is received depends on its transmitted intensity. Before, progressing to receiver module design we need to focus on basic functionality on how echo receiver works and factors it depends on. From basic, Sonar equation [32] echo level can be detected by providing other parameters are solely known.

$$E_L = S_L - 2T_L + T_S - N_L + N_{ag}$$

Here,

$E_L$  - echo level

$S_L$  - Source level

$T_L$  - Transmission or propagation loss

$N_L$  - Total noise

$T_S$  - Target strength

Reflected echo from different object carries its own characteristics. Not essentially reflecting objects are our desired targets. Our desired target is river bed, hence other echoes are noise. Target echo should reflect from way down the river bed and return to transducer. Transducer will listen to echo and enumerate distance measurement based on 'time of flight' equation. Spectrum analysis, is what has been carried out to distinguish river bank. Isolating reflecting objects is difficult as individual object imposes its own trait. Rigid object reflects echo better than flimsy object, due to its composite structure. Identifying texture of the soil is another challenge as it does not persistently remain the same. Echo might even interact with incident sound wave to produce a complex waveform which is strenuous to unfold. Choice of filter circuit (peak detection) is crucial in such cases, where it is required to isolate different targets from received reverberation. Transmitted pulse bandwidth must match with that of receiver's. The reason we are using 200 kHz band-pass filter at initial stage of receiver module [34].

Before progressing towards envelope detection design, we will first look into how basic peak detector works. Peak or envelope detector unfolds maximum magnitude of a signal over certain duration.

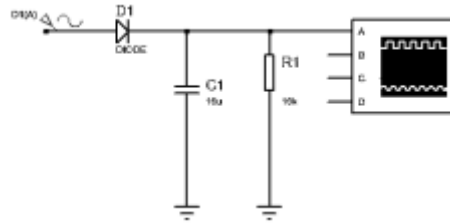


Fig.4.18: Single Stage Peak detector

Discharged rate can be calculated from time constant ' $\tau$ ' which obviously depends on ' $RC$ ' parameter.

$$\tau = R_1 * C_1$$

Variation of output voltage, which determines the upper and lower limit of envelope, where  $V_{peak}$  is the maximum amplitude voltage, ' $f$ ' is the input signal frequency, and ' $\tau$ ' is the discharge time constant.

$$\Delta V = \frac{V_{peak}}{f * \tau}$$

The above equation is for a pure input signal (example sinusoid). In our case we expect pulsating wave with greater variation. Variation in amplitude is due to different depth measurement. Such pulsating or modulating signal rather follows time variant properties [33].

$$V_{drop} = V_{peak} * \exp\left(-\frac{t}{\tau}\right)$$

Value of time constant affects ripple factor. In order to reduce ripple,  $\tau$  must be as large as possible. We implemented a two-stage peak detector, where the first amplifier ( $A_1$ ) works to charge capacitor to peak value and second amplifier ( $A_2$ ) acts as output buffer. Moreover, fluctuation of input and output impedance is reduced by  $A_1$  and  $A_2$  respectively. Using the equation below, lower frequency can be calculated which gives a measure of ripple voltage.

$$f_o = \frac{1}{R_3 * C_1 * \ln\left(\frac{V - V_o}{V - V_c}\right)}$$

Here,

$V$ -Capacitor discharge voltage

$V_c$ - Minimal voltage on capacitor

$V_o$ -Initial Charge on Capacitor

**Simulated Circuit:**

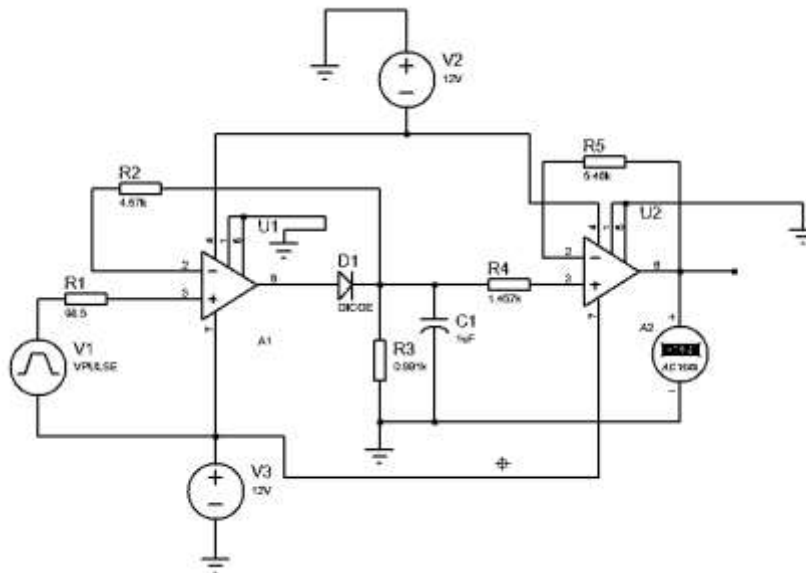


Fig.4.19: Two-stage Peak detector circuit Simulation [created in proteus]

**Circuitry:**

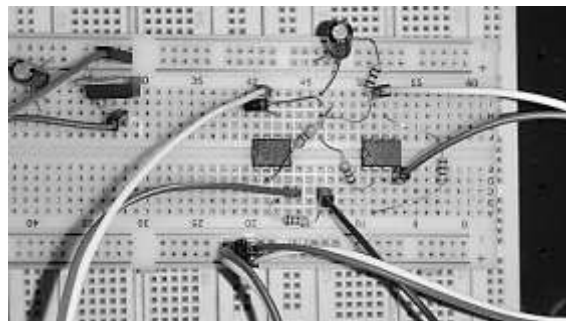


Fig.4.20: Two-stage peak detector

**Oscilloscope Waveform:**

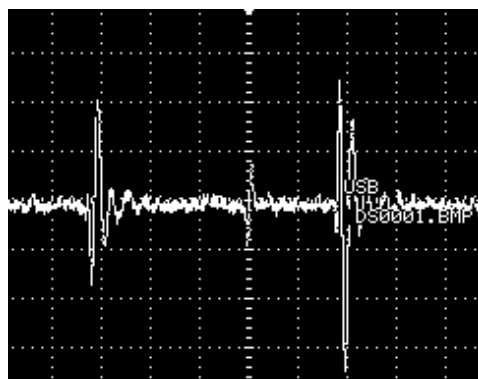


Fig.4.21: Two stage peak detector output waveform

**Design value:**

$R_1 = 98.5 \Omega$	$R_3 = 0.991 \text{ k}\Omega$	$R_5 = 5.46 \text{ k}\Omega$
$R_2 = 4.57 \text{ k}\Omega$	$R_4 = 1.457 \text{ k}\Omega$	$C_1 = 1\mu\text{F}$



### 4.2.2.3. Comparator (Analog-to Digital Conversion):

#### *Non-inverting Comparator circuit*

Comparator circuit basically compares input voltage signal with the reference or threshold voltage set. From a fixed voltage level it determines which signal is the greatest. Echo detector ( $V_{\text{echo-detect}}$ ) output is fed into non-inverting comparator input. DC ref-voltage is applied to inverting terminal. Comparison in voltage is done between output voltage from echo-detector and DC-ref voltage. If  $V_{\text{peak-detect}} > V_{\text{ref}}$ , output voltage of comparator will be in positive saturation region implying that non-inverting voltage  $V_+$  is greater than the inverting voltage.

In other case if  $V_{\text{peak-detect}} < V_{\text{ref}}$ , output voltage transits from positive saturation region to negative saturation, resulting in non-inverting voltage  $V_+$  being less than the inverting voltage [35].

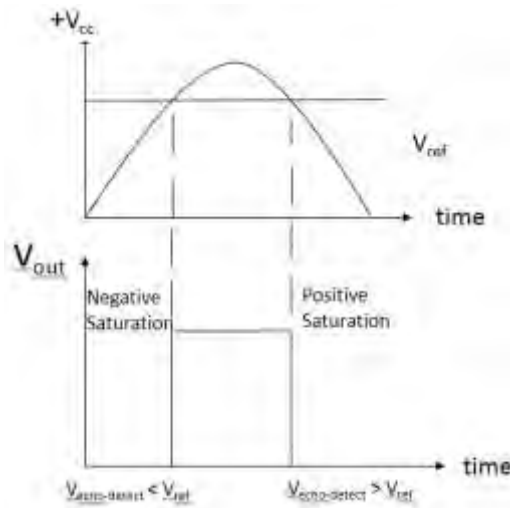


Fig.4.22: Saturation at different comparator region [created in MS Powerpoint]

Since MCU better works with digital or quantized voltage level. This stage of our circuit converts pulsating sinusoid output from echo-detector to discrete pulse. Output from comparator is our desired digital signal. Where the voltage level varies in proportion to distance measured. This circuit was calibrated using different threshold voltage. Setting up the required reference voltage was the key parameter needed to alter. After several trial and error simulation and hardware adjustments. This was deduced that since maximum distance required to measure ' $d_{\text{max}} \leq 50\text{m}$ ' and our maximum amplified echo voltage detected at this distance was 4.88V. Voltage above this is out of our interest. There is no point in comparing voltage exceeding this. We needed two comparator circuit which can compares two different threshold level between 0V and 5V.  $V_{\text{ref}}$  comes after a 2.154k $\Omega$  resistor, due some voltage drop across resistor, V2 was set to 1V and 6V in comparator 1 and comparator 2 respectively. Finally, output of this two comparator circuit is passed through a summing amplifier. Due to its simplicity in configuration, it was not shown in the circuit simulation. A single stage 741 operational amplifier was used to add two comparator output. Summing amplifier's output retains total digital signal encoding underwater depth measured value less than 50m real distance.

**Simulated Circuit:**

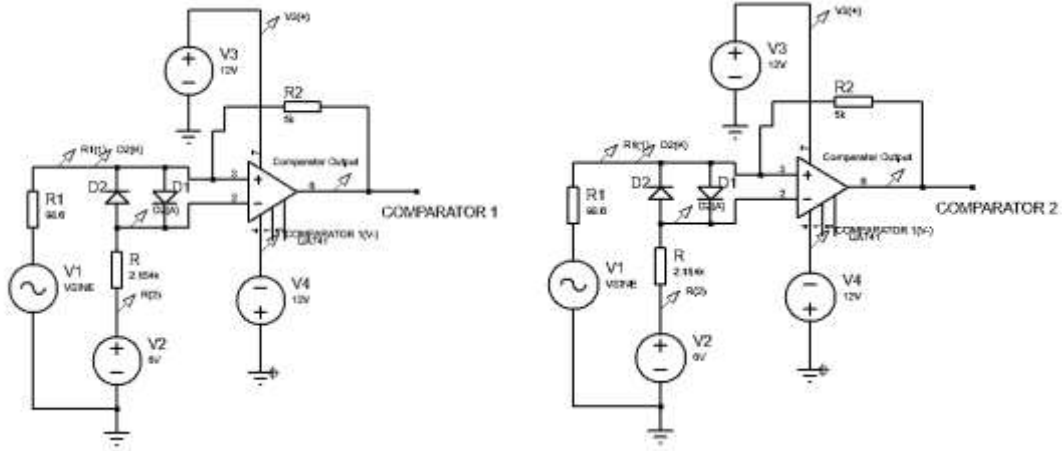


Fig.4.23: Simulation Model Comparator 1 and Comparator 2 [created in proteus]

**Circuitry:**

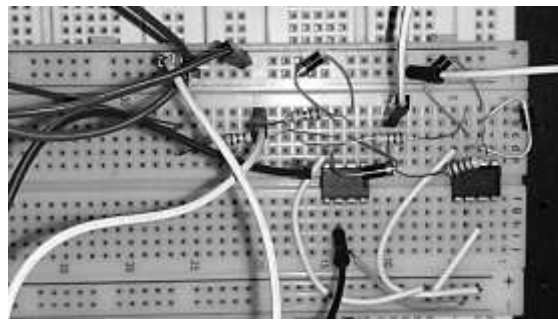


Fig.4.24: Two stage comparator

**Oscilloscope Waveform:**

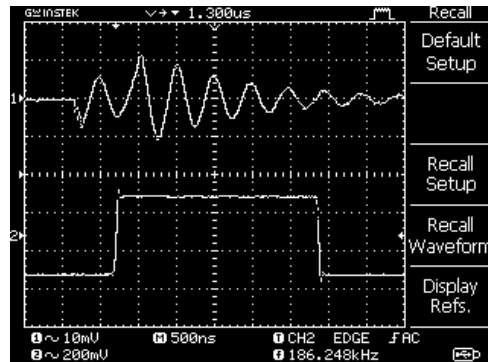


Fig.4.25: Echo and Comparator Output

Lower and upper threshold voltage was calculated from equation,

$$V_{TH} = (R_1 + R_2) * V_{ref} - \frac{R_1 V_{oL}}{R_2}$$

$$V_{TL} = (R_1 + R_2) * V_{ref} - \frac{R_1 V_{oH}}{R_2}$$

### 4.3.Mechanical Module Design:

The underwater ultrasonic transducers needed to be submerged for perception. Again, we were adamant to use the servo motor due to its ease of use with angular movements. But we could not find an underwater servo motor. Thus, we came up with a problem where we had to deal with the servo being overboard the vehicle and the sensors submerged under water. This required us to design a mechanical system that would hold the sensors under water and also smoothen the servo synchronization with the sensors used. We therefore used a 4-bar linkage mechanism to perform the work. This enabled us not only to put the system under water but also solved the problem of changing the direction of the angle for tone burst under the water surface according to the necessity of the user.

#### 4.3.1.Linkage:

Linkages are perhaps the most fundamental class of machines that humans employ to turn thought into action. From the first lever and fulcrum, to the most complex shutter mechanism, linkages translate one type of motion into another.

A linkage, or kinematic chain, is an assembly of links and joints that provide a desired output motion in response to a specified input motion. A link is a nominally rigid body that possess at least 2 nodes. A node is an attachment point to other links via joints. The order of a link indicates the number of joints to which the link is connected (or the number of nodes per link). There are binary (2 nodes), ternary (3 nodes), and quaternary (4 nodes) links. A joint is a connection between two or more links at their nodes, which allows motion to occur between the links. Now, let us move to a proper definition of linkage and the generalized equations. Linkage is a system of links connected at joints with rotary or linear bearings

– Joint (kinematic pairs): Connection between two or more links at their nodes, which allows motion to occur between the links

– Link: A rigid body that possess at least 2 nodes, which are the attachment points to other links

Degrees of Freedom (DOF):

– The number of input motions that must be provided in order to provide the desired output, OR

– The number of independent coordinates required to define the position & orientation of an object

– For a planar mechanism, the degree of freedom (mobility) is given by Gruebler's Equation:

$$DOF = 3(n - 1) - 2f_1$$

– n = Total number of links

– f<sub>1</sub> = Total number of joints

In our case, the 4-bar linkage mechanism and its degree of freedom is calculated as,

$$DOF = 3(4 - 1) - 2 * 4 = 1$$

### 4.3.2. Proposition of Mechanical Module:

In our system, the linkage is present in the central part of the system as can be seen in the figure below:

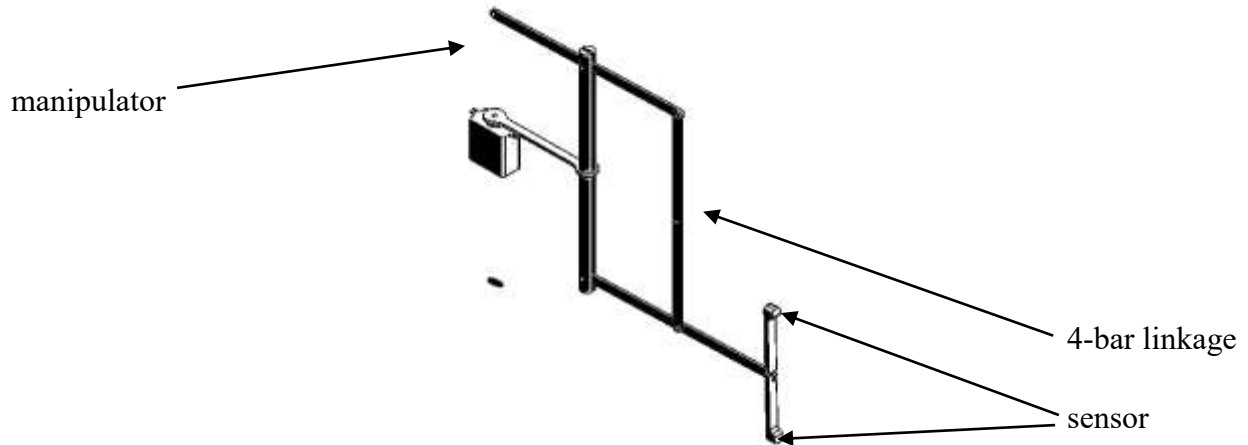


Fig.4.26: Servo mounted with presumed design of sensors in front (Designed in SolidWorks 2014).

The servo remains fixed to the vehicle at its base and will be kept well overboard while the upper bar will be used for controlling the DOF. The 4-bar linkage works as the connector to enable the DOF while the sensors remain fixed to the lower bar. The bidirectional movement will control the sensors to form an angle with the surface of water as they remain submerged.

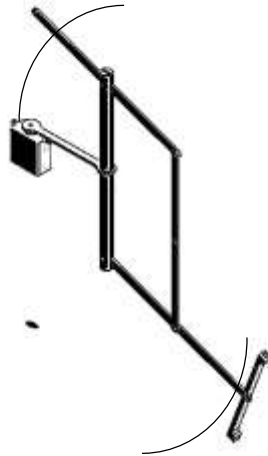


Fig.4.27: 1-DOF of the Mechanical Module [Designed in SolidWorks 2014]

The chalked out design will be made of aluminium to ensure light weight but not too soft to break off during high turbidity in the water surface. It may also be coated with water resistant to avoid rusting.

#### 4.4. Algorithm Design:

At first using the pulseIn() function of the arduino we calculate the distance in meter and then send it to the processing software using the Serial Port. Then, in the processing software we read the value that was send by the arduino and initially store the values in an array and after that store them in an Arraylist so that when the arrays are cleared they are not lost. Afterwards, using the beginShape() function we join the vertices in 3D using the values stored in the arraylist and form the surface. We have shown the surface in 15 columns and 5 rows. During the first loop we initially draw the surface of the first loop and after that we draw the surface in 2 rows at a time in addition to the first loop which goes to the back and as a result it seems like moving. After the end of 5 rows one loop is used for resetting. Then for differentiating between the distances we use the functions color1(), color2(), color(3), color(4), color(5), color(6), color(7) and color(8). For understanding and drawing of the spectrum the spectrum() function is used. This whole process goes in a loop within the draw() function until it is stopped.

#### 4.5. Software Calibration:

The codes that were written on arduino and on Processing was tested using a real life test case with a rather commonly used ultrasonic sensor for general understanding. The HC – SR04 ultrasonic sensor was used with the software on a regular rectangular shaped terrain of maximum length of 14 cm. The terrain received were satisfactory.

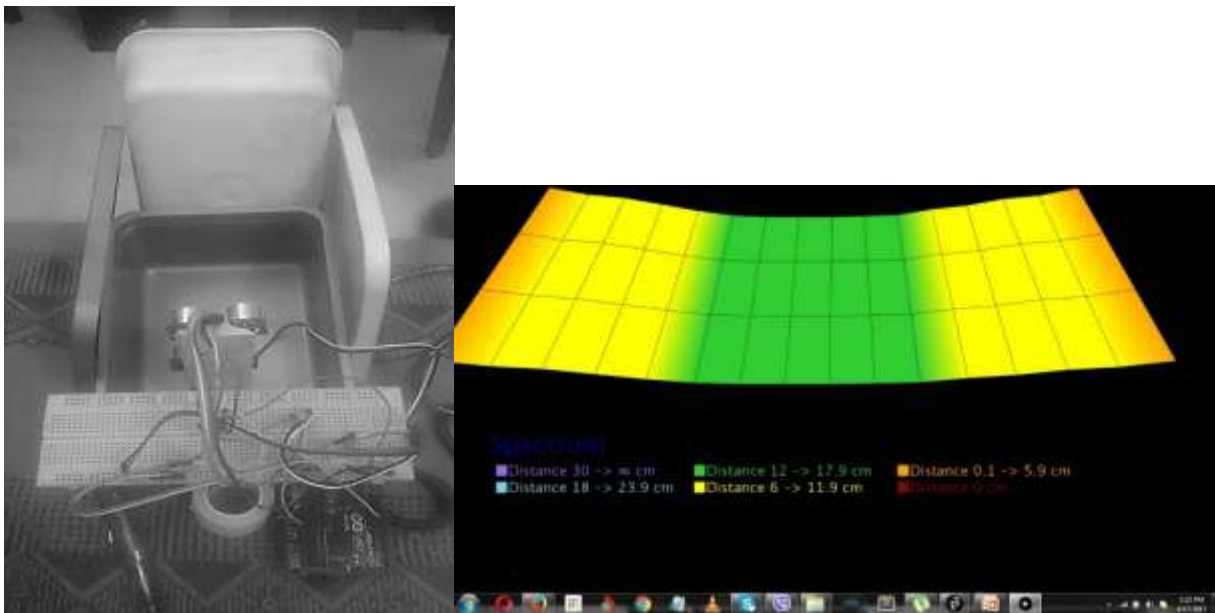


Fig.4.28 : Test case and Software Output (Test case) [created in processing 3.2.3]

The output as seen was calibrated at lower range than the actual transducer used. The td0200ka transducer ranges from 0.6m to 50m whereas the HC – SR04 has a range of 0.2cm to 4m. The calibration proved successful creation of approximate terrain.

## Chapter 5

### Experimentation and Result Analysis

#### 5.1.Lab Testing:

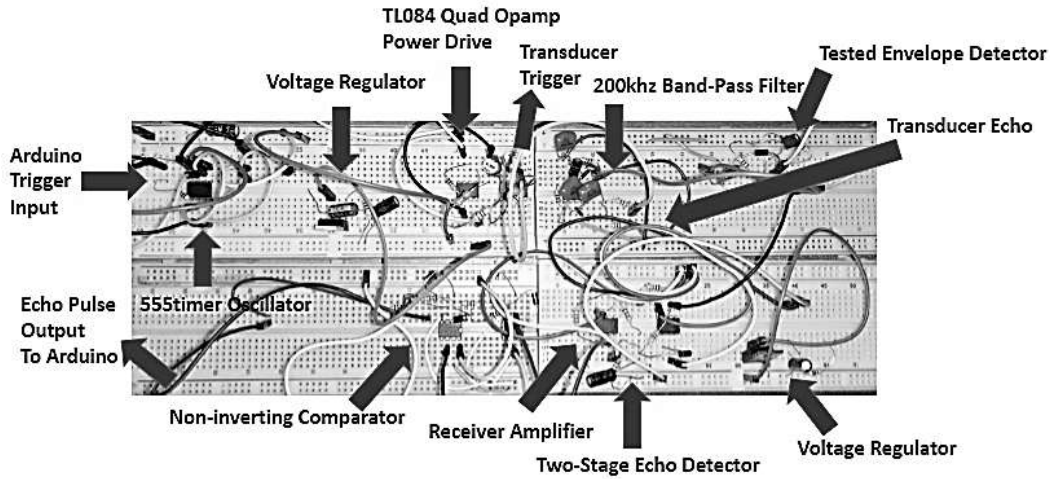


Fig.5.01:Complete Module Circuitry

In the lab, the complete circuit was triggered and the triggering and echo waveforms were tested. The probes were checked on the trigger and echo pins of the circuit after connections and the waveform was obtained in air.

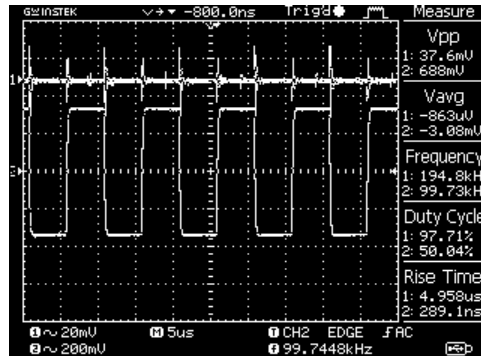


Fig.5.02: Transmission and Echo

Tests were conducted on how the transducer module perceived distance in air. The tabulation data shows the expected output and the obtained output from the serial monitor of the arduino software and respective voltages of the echo and trigger pin.

#### 5.01.Tabulation for Voltage level and corresponding Distances (air)

$V_{\text{Trigger}}$ mV	$V_{\text{Echo}}$ mV	Actual Distance m	Distance on Monitor m	Error %
90	830	1	1.26	74%
93	1050	2	2.21	89.5%

94	1410	5	6.14	77.2%
94	1540	6	6.37	93.8%
97	1710	8	9.19	85.13%
99	1810	10	11.51	84.9%
98	1960	12	13.06	91.2%

## 5.2. Field Testing:

A small scale field testing was conducted on a minor water body to define if the system actually worked at large. The test case was shallow and had a maximum depth of about approximately 4m, according to information received. The boat was just run in a straight line and no servo was connected to the sensor due to accommodation problem. The output received was just one line as data was perceived vertically, whereas, the actual data perception will be horizontal. The test case was a small pond being made ready for fish culture situated in Plot – 36, Road – 14, Nobinagar Housing, Bosilla, Mohammadpur, Dhaka. The first case didn't show any change in terrain as the change was very meagre in comparison to the terrain range, which was about 50m. then we changed the scale to one-fifth of the actual terrain so that the terrain change could be understood and emphasized properly.

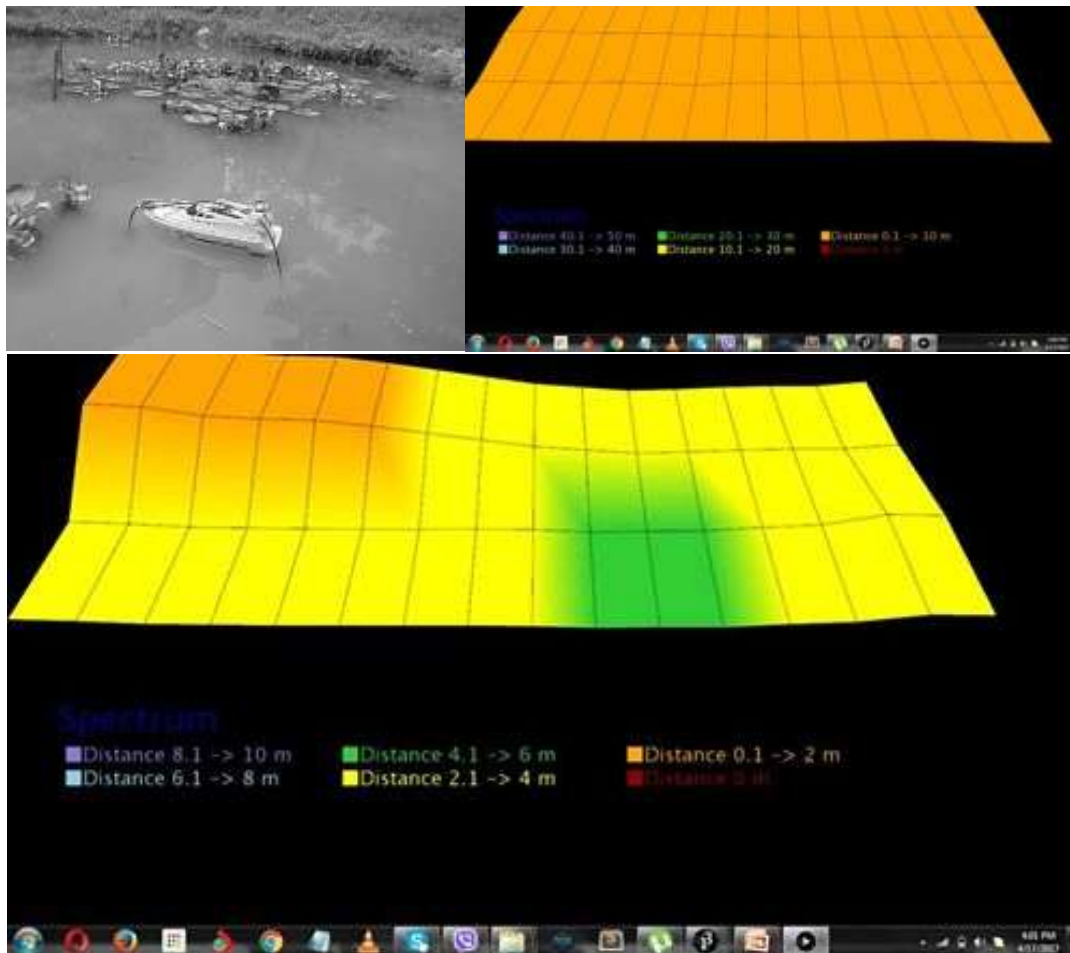


Fig.5.03: Test case and Software Output (Field test) [created in processing 3.2.3]

The output shows the terrain that was received from under the boats and thus only gave depths and shapes underneath.

### **5.3. Analysis:**

As the table suggests, the efficiency is not as accurate as expected. The reason behind the accuracy problem may be because the module was built on breadboard by unprofessional hands and could give better output when done on Printed Circuit Board by professionals. Moreover, the transducer being underwater, they were tested on air and might give better results underwater. At least the terrain received is approximate and almost a satisfactory 3D surface can be seen.



## Chapter 6

### Conclusion

To sum up, the complete module that has been designed from scratch under adverse conditions with amateur hands on breadboard and may lack accuracy but the perception of underwater surface for mapping will define a terrain to avail an approximate solution to safe navigation. The terrain will present to the driver a distance based spectral map to remain in safe regions on water and avoid being trapped on banks or colliding with other objects when visual is compromised.

This project could be made professionally and thus reduce module size using nano-sized components on PCB for better results.

#### **6.1.Further Development:**

The project has potential. Increasing accuracy and efficiency would be a worthy challenge. PCB can be made to check for better outcomes. The industrial preparation of the module and promotion for use could help improve situations in the country and also in places of need. The software could also be developed with a more user friendly GUI. In arduino and processing 3.2.3 softwares memory has been a big challenge. The project will be tested on Raspberry Pi. The software processing 3.2.3 has a poor reaction time and thus image mapping image could suffer at times. A newer, faster software could be used for better results. Further down the line, using a database to store the distance data, creating and updating of the data on GPS could give an almost permanent solution to navigation and routing.

## Chapter 7

### Project Management

#### 7.1. Project Management:

Project management is a very important issue for successful completion of a project. It is the process and activity of planning, organizing, motivating and controlling resources, procedures and protocols in achieving specific goals. As hardware projects require cost allocation and budgeting as well as time management, the process is necessary for final year projects. A Gantt chart was developed and we tried to follow the schedule.

#### 7.2. Project Schedule:

Project scheduling was done at almost the beginning of the project and approximate schedules were maintained. Though the last minutes preparations are always panicking and menacing. Gantt charts have been supplied in appendix D as divided into 3 semesters – Summer, Fall and Spring.

#### 7.3. Cost Estimation

##### 7.01. Tabulation for Cost Estimation

Component	Unit	Unit Price	Cost BDT
TD0200ka underwater ultrasonic transducer	2	\$50	8000/-
R/C SERVOS HITECH/FUTABA	1	£12	1219/-
Inductors	4	BDT 36	144/-
Breadboard	4	BDT 240	960/-
TL084 Opamp	2	BDT 240	480/-
LM358	4	BDT 220	880/-
Breadboard Trim Pot	6	BDT 120	720/-
Total cost			12403/- (approx.)

## References:

1. Bangladesh Regional Waterway Transport Project Charles Kunaka Senior Trade Specialist Global Product Specialist. (n.d.). Retrieved from [http://www.cemm.ca/Documents/pdf/mission\\_washington/7-CharlesKunaka\\_BangladeshRegionalWaterwayTransportProject.pdf](http://www.cemm.ca/Documents/pdf/mission_washington/7-CharlesKunaka_BangladeshRegionalWaterwayTransportProject.pdf)
2. Ref: World Bank - BANGLADESH TRANSPORT POLICY NOTE 2009, Bangladesh Government Economic Review - 2010 English Edition, World bank - Revival of Inland Water Transport, Bangladesh BIWTA, BIWTC. (n.d.). Retrieved from <http://dlca.logcluster.org/download/attachments/852989/Bangladesh%20Waterways%20Assessm ent.doc?version=1&modificationDate=1380646251000&api=v2>
3. Sakalayan, Q. H. (2006). Non-conventional ferry safety and the potentiality of inland waterways for multimodal transportation : a comparative analysis for the betterment of Bangladesh's situation. *World Maritime University Dissertations. Paper 343*. Retrieved from [http://commons.wmu.se/cgi/viewcontent.cgi?article=1342&context=all\\_dissertations](http://commons.wmu.se/cgi/viewcontent.cgi?article=1342&context=all_dissertations)
4. Saha, B. K. (n.d.). Daulotdia-Paturia ferry services disrupted again. Retrieved from <http://www.banglanews24.com/national/article/5800/Daulotdia-Paturia-ferry-services-disrupted-again>
5. New Age – Dense fog disrupts ferry service on Shimulia-Kawrakandi route. (n.d.). Retrieved from <http://archive.newagebd.net/197992/dense-fog-disrupts-ferry-service-on-shimulia-kawrakandi-route/>
6. New Age – Fog disrupts ferry services. (n.d.). Retrieved from <http://archive.newagebd.net/75507/fog-disrupts-ferry-services/>
7. New Age – Ferry service between Shimulia, Kawrakandi suspended. (n.d.). Retrieved from <http://archive.newagebd.net/150796/ferry-service-between-shimulia-kawrakandi-suspended/>
8. Bus movement at Daulatdia-Paturia ferry ghats halted for 72 hours | Dhaka Tribune. (n.d.). Retrieved from <http://archive.dhakatribune.com/bangladesh/2013/sep/02/bus-movement-daulatdia-paturia-ferry-ghats-halted-72-hours#sthash.vS0T4onb.dpuf>
9. 2009 Bangladesh ferry accident - Wikipedia. (n.d.). Retrieved April 15, 2017, from [https://en.wikipedia.org/wiki/2009\\_Bangladesh\\_ferry\\_accident](https://en.wikipedia.org/wiki/2009_Bangladesh_ferry_accident)
10. Tadiou, K. M. (2014). Computer Vision - The Future of Human Evolution. Retrieved from <http://futurehumanevolution.com/artificial-intelligence-future-human-evolution/artificial-intelligence-computer-vision>

11. VanMiddlesworth, M. Toward autonomous underwater mapping in partially structured 3D environments. Master of science. Department of Electrical Engineering and Computer Science, Massachusetts Institute of Technology. 2014.
12. Zhong, C. H. (2015). *Low cost autonomous underwater 3D mapping* (Doctoral dissertation, Teknologi Malaysia, Malaysia). Retrieved from [http://ent.library.utm.my/client/en\\_AU/main/search/detailnonmodal/ent:\\$002f\\$002fSD\\_ILS\\$002f0\\$002fSD\\_ILS:858575/ada?qu=Oman&qf=ITYPE%09Material+Type%091%3ACLS\\_THESIS%09Closed+Access+Thesis&ic=true&ps=300](http://ent.library.utm.my/client/en_AU/main/search/detailnonmodal/ent:$002f$002fSD_ILS$002f0$002fSD_ILS:858575/ada?qu=Oman&qf=ITYPE%09Material+Type%091%3ACLS_THESIS%09Closed+Access+Thesis&ic=true&ps=300)
13. Kinneging, N., Snellen, M., Eleftherakis, D., Simons, D., Mosselman, E. and Sieben, A. River bed classification using multi-beam echo-sounder backscatter data. Dijk van, T., ed. Hydro12 - Taking care of the sea. Rotterdam: Hydrographic Society Benelux. 2012. ISBN 9036534704.
14. Kuperman, W. and Roux, P. Underwater Acoustics, Springer New York, book section 5. 2007. ISBN 978-0-387-30446-5, 149–204.
15. Feurer, D., Bailly, J.-S., Puech, C., Le Coarer, Y. and Viau, A. A./ Very-high resolution mapping of river-immersed topography by remote sensing. Progress in Physical Geography, 2008. 32(4): 403–419. ISSN 0309-1333.
16. Instruments, L. C. S. Multibeam Sonar Theory of Operation. Report. L3 Communications SeaBeam Instruments. 2000. Most relevant to SeaBeam 2100 series sonars.
17. Gleason, A., Preston, J. and Bloomer, S. Reproducibility of single-beam acoustic seabed classification. OCEANS 2009, MTS/IEEE Biloxi – Marine Technology for Our Future: Global and Local Challenges. Biloxi, MS: IEEE. 2009. 1–5.
18. Wang, Q. Underwater object localization using a biomimetic binaural sonar. Master of science in oceanographic engineering. Department of Ocean Engineering, Massachusetts Institute of Technology. 1999.
19. Haming, K. P. G. The structure-from-motion reconstruction pipeline - a survey with focus on short image sequences. Kybernetika, 2010. 46(5): 926–937.
20. Mahacek, P., Berk, T., Casanova, A., Kitts, C., Kirkwood, W. and Wheat, G. Development and initial testing of a SWATH boat for shallow-water bathymetry. OCEANS 2008. Quebec City, QC: IEEE. 2008. 1–6.
22. Transducers - The Ultrangroup. (n.d.). Retrieved from <http://www.ultrangroup.com/index.php/products/transducers/>
23. Interactive plot of radiation patterns in polar format - MATLAB. (n.d.). Retrieved from <https://www.mathworks.com/help/phased/ref/polarpattern-class.html#bvcpemr>

24. Transducer cone angles and their coverage area [Archive] - Walleye Message Central. (n.d.). Retrieved from <http://www.walleyecentral.com/forums/archive/index.php/t-18678.html>
25. Characteristics of Piezoelectric Transducers. (n.d.). Retrieved from <https://www.nde-ed.org/EducationResources/CommunityCollege/Ultrasonics/EquipmentTrans/characteristicspt.htm>
26. Retrieved from <http://web.mit.edu/2.75/fundamentals/FUNdaMENTALs%20Book%20pdf/FUNdaMENTALs%20Topic%204.PDF>
27. Adul Zehra Abd, A. H. (2014). *Design and simulation of 4th order active bandpass filter using multiple feed back and Sallenkey topologies* , 22.
28. Rodriguez, M. G., Alvarez, J. G., Yanez Y., Garcia-Hernandez, M. J., Salazar J., Turo A., & Chavez, J. A. (2009). *Low Cost Matching Network for Ultrasonic Transducers*.
29. *On The Design Of Matching Systems For Piezo Elements*. (n.d.).
30. Rosu I. (n.d.). *Impedance Matching*. Retrieved from <http://www.qsl.net/va3iul/>
31. M.G.Rodrigue, J. G.Alvarez, Y. Yanez, M.J. Garcia-Hernandez, J. Salazar, A. Turo, J.A. Chavez: *Low Cost Matching Network for Ultrasonic Transducers*
- 32 HODGES, R. P. (2010). *UNDERWATER ACOUSTICS ANALYSIS, DESIGN AND PERFORMANCE OF SONAR*.
- 33 Dosu D. (n.d.). *Op Amp, Rectifier, Peak Detector and Clamps*.
- 34 Nguyen, M. T. (2004). *Design of an Active Acoustic Sensor System for an Autonomous Underwater Vehicle* (Doctoral dissertation, The University of Western Australia, Australia).
35. 741 IC Op-amp comparator circuit diagram,schematic, design,working. (n.d.). Retrieved from <http://www.circuitstoday.com/op-amp-comparator>
36. Schwartz, M. (n.d.). Reflection, Transmission and Impedance. Retrieved from <http://users.physics.harvard.edu/~schwartz/15cFiles/Lecture9-Impedance.pdf>
37. TDC1000 Ultrasonic Sensing Analog Front End (AFE) for Level Sensing, Flow Sensing, Concentration Sensing, and Proximity Sensing Applications. (n.d.). Retrieved from [http://www.tij.co.jp/product/jp/TDC1000-Q1/datasheet/application\\_and\\_implementation](http://www.tij.co.jp/product/jp/TDC1000-Q1/datasheet/application_and_implementation)
38. patternCustom. (n.d.). Retrieved from <https://www.mathworks.com/help/antenna/ref/patterncustom.html>

39. Waite, A. (n.d.). Sonar for Practising beginners. JOHN WILEY & SONS, LTD.
40. Hodges, R. (2010). UNDERWATER ACOUSTICS ANALYSIS, DESIGN AND PERFORMANCE OF SONAR. WILEY.
41. Ultrasonic Transducers Technical Notes. (n.d.). OLYMPUS.
42. Laxamana.N SONAR Technology for Fish Finders
43. Piezoelectric Ceramics OPERATING PRINCIPLES OF PIEZOELECTRIC CERAMICS. (2013).

## Appendix A: Components Used

### Oscillator Stage

- i) NE555 timer: [www.ti.com/lit/ds/symlink/lm555](http://www.ti.com/lit/ds/symlink/lm555)
- ii) Resistor, Capacitor:
- iii) Transistor BC560C: <http://www.onsemi.com/pub/Collateral/BC560C-D.PDF>

### Voltage Regulator

<http://www.ti.com/lit/ds/symlink/lm317.pdf>

### Power Drive/Receiver Amplifier:

- i) TL084: <http://pdf1.alldatasheet.com/datasheet-pdf/view/28804/TI/TL084CN.html>
- ii) Potentiometer, Capacitor:
- iii) Buck-boost:  
Power MOSFET IRF540N: <http://www.vishay.com/docs/91021/91021.pdf>  
IRF9610: <http://www.datasheets360.com/part/detail/irf9610/6975304709353999446/?alternatePartManufacturerId=0>

### Impedance Matching:

- i) Inductor
- ii) Transformer 220V-12V, 50Hz

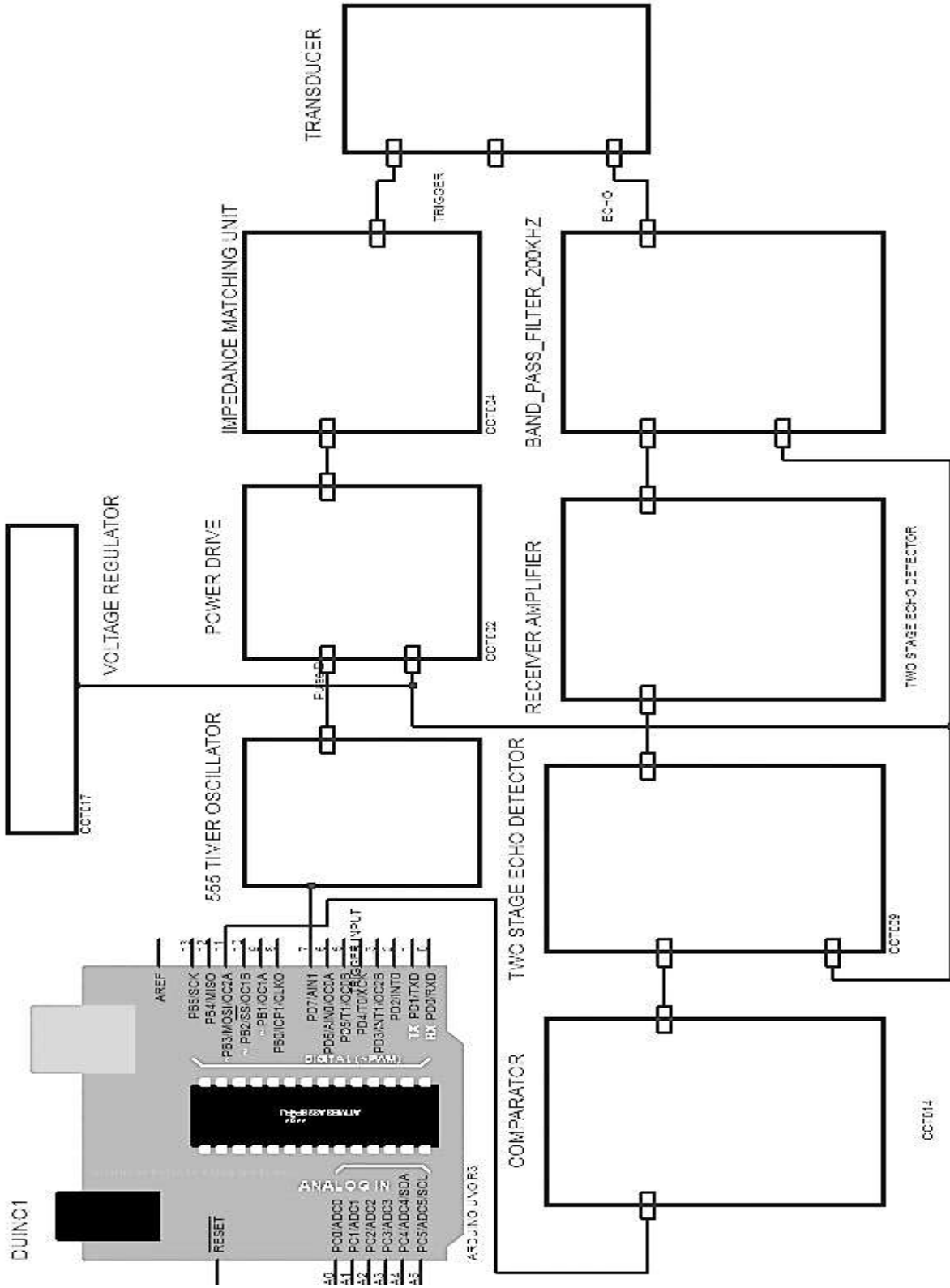
### Band Pass, Echo detector, Comparator:

LM358: <http://www.ti.com/lit/ds/symlink/lm158-n.pdf>  
SCHOTTKY BARRIER RECTIFIER: <https://www.diodes.com/assets/Datasheets/ds23001.pdf>  
Diode: <https://www.diodes.com/assets/Datasheets/ds23001.pdf>  
TL084: <http://pdf1.alldatasheet.com/datasheet-pdf/view/28804/TI/TL084CN.html>

## Appendix B: Transducer Datasheet

<http://chinaultrasound.com/product/200-khz-ultrasonic-transducer-depth-measurement-td0200ka/>

## Appendix C: Signal Flow Diagram





## Appendix D: Gantt chart

### Summer 2016

Week	1	2	3	4	5	6	7	8	9	10	11	12	13
Title proposal													
Analysis of topic													
Research on existing technologies													
Literature review													
Transducer selection													
Programming design													
Report submission													

### Fall 2016

Week	1	2	3	4	5	6	7	8	9	10	11	12	13
Transducer purchase													
Transducer test & parameter evaluation													
Simulation design													
Circuit simulation													
Hardware purchase													
Circuit design													
Circuit lab simulation													
Report submission													

### Spring 2017

Week	1	2	3	4	5	6	7	8	9	10	11	12	13
Integration													
Program calibration													
Lab testing													
Site testing (full system)													
Report writing													
Presentation													
Report submission													

## Appendix D: Codes

### Block 1: Arduino Code

```
// Includes the Servo library
#include <Servo.h>

// Defines Trig and Echo pins of the td0200ka
const int trigPin1 = 10;
const int echoPin1 = 11;

const int trigPin2 = 8;
const int echoPin2 = 12;

long duration1;
int distance1;
long duration2;
int distance2;

Servo myServo1;

void setup() {
  pinMode(trigPin1, OUTPUT); // Sets the trigPin as an Output
  pinMode(trigPin2, OUTPUT); // Sets the trigPin as an Output
  pinMode(echoPin1, INPUT); // Sets the echoPin as an Input
  pinMode(echoPin2, INPUT); // Sets the echoPin as an Input
  Serial.begin(9600);
  myServo1.attach(9); // Servo motor attached on pin 9
}

void loop() {

  for(int i=15;i<=155;i=i+10
  ){
  myServo1.write(i);

  delay(250);
  distance1 = calculateDistance1(); // Calls function for measuring distance
  distance2 = calculateDistance2(); // Calls function for measuring distance
```

```

Serial.print(distance1); // Sends the distance value into the Serial Port
Serial.print(","); // Sends addition character right next to the previous value needed later in the
Processing IDE for indexing
Serial.print(distance2); // Sends the distance value into the Serial Port
Serial.print("."); // Sends addition character right next to the previous value needed later in the
Processing IDE for indexing
}
}

```

```

// Function for calculating the distance measured

```

```

int calculateDistance1(){

digitalWrite(trigPin1, LOW);
delayMicroseconds(2);
// Sets the trigPin HIGH for 10 micro seconds
digitalWrite(trigPin1, HIGH);
delayMicroseconds(10);
digitalWrite(trigPin1, LOW);
duration1 = pulseIn(echoPin1, HIGH); // Reads the echoPin, returns the sound wave travel time
in microseconds
distance1= (duration1*0.1484/2)/100;
return distance1;
}

```

```

int calculateDistance2(){

digitalWrite(trigPin2, LOW);
delayMicroseconds(2);
// Sets the trigPin HIGH for 10 micro seconds
digitalWrite(trigPin2, HIGH);
delayMicroseconds(10);
digitalWrite(trigPin2, LOW);
duration2 = pulseIn(echoPin2, HIGH); // Reads the echoPin, returns the sound wave travel time
in microseconds
distance2= (duration2*0.1484/2)/100;
return distance2;
}

```

## Block 2: Processing 3.2.3 Code

```
import processing.serial.*; // imports library for serial communication
import java.awt.event.KeyEvent; // imports library for reading the data from the serial port
import java.io.IOException;
Serial myPort; // defines Object Serial

int coloumns = 15;
int rows = 5;
int max = 50;

int pin = -15;
int q = 0;

int k = 0;
int m = 0;
int n = 0;
boolean check = false;

String distance1="";
String distance2="";
String data="";
int iDistance1;
int iDistance2;
PFont orcFont;
int index1 = 0;

ArrayList <Float> a1 = new ArrayList<Float>();
ArrayList <Float> b1 = new ArrayList<Float>();

ArrayList <Float> a2 = new ArrayList<Float>();
ArrayList <Float> b2 = new ArrayList<Float>();

float[] terrain1 = new float[64];
float[] terrain2 = new float[64];
int scl = 50;
int scale = 100;
float scaling = 4;

void setup(){
  fullScreen(P3D);
```

```

    smooth();
myPort = new Serial(this,"COM12", 9600);
myPort.bufferUntil('.');
orcFont = loadFont("OCRAExtended-30.vlw");

    background(0);
}

void draw() {
    background(0);

    pin = pin + 15;
    q = q + 15;

    spectrum();
    noFill();
    translate(0,100) ;
    rotateX(PI/4);

//Taking distance input from arduino
for(int p = pin ; p < q ; p++){
    if(iDistance1 > max){
        iDistance1 = 50;
    }
    if(iDistance2 > max){
        iDistance2 = 50;
    }
    terrain1[p] = (max - iDistance1)*3;
    terrain2[p] = (max - iDistance2)*3;
    delay(262);
}

//Store the values in an Arraylist

    if(k < rows){

        for(int i = 0; i < coloumns; i = i + 1){

            // For even
            if(k % 2 == 0){

                a1.add(terrain1[m]);

```

```

b1.add(terrain2[m]);
b1.add(terrain2[m+1]);
a1.add(terrain1[m+1]);

m = m + 1;
check = false;
}

//For odd
else{
a1.add(terrain1[n+coloumns+1]);
b1.add(terrain2[n+coloumns+1]);
b1.add(terrain2[n+coloumns+2]);
a1.add(terrain1[n+coloumns+2]);

b2.add(terrain2[n+coloumns+1]);
a2.add(terrain1[n]);
a2.add(terrain1[n+1]);
b2.add(terrain2[n+coloumns+2]);

n = n + 1;
check = true;
}
}
if(check == true){
k = k + 1;
}
moving(k);

if(check == false){
m = m + 1;
}
else{
n = n + 1;
}
}
else if(k >= rows){
k = -1;
m = 0;
n = 0;
pin = -15;
q = 0;
}

```

```

    check = false;
    a1.clear();
    b1.clear();
    a2.clear();
    b2.clear();
}
k = k+1;
}

```

```

void serialEvent (Serial myPort) { // starts reading data from the Serial Port
  // reads the data from the Serial Port up to the character '.' and puts it into the String variable
  "data".

```

```

  data = myPort.readStringUntil('.');
  data = data.substring(0,data.length()-1);

```

```

  index1 = data.indexOf(","); // find the character ',' and puts it into the variable "index1"
  distance1= data.substring(0, index1); // read the data from position "0" to position of the
  variable index1 or thats the value of the angle the Arduino Board sent into the Serial Port
  distance2= data.substring(index1+1, data.length()); // read the data from position "index1" to
  the end of the data pr thats the value of the distance

```

```

  // converts the String variables into Integer
  iDistance1 = int(distance1);
  iDistance2 = int(distance2);
}

```

```

//Creates the moving surface body
void moving(int p){

```

```

stroke(0);
fill(0,250,0);

```

```

boolean checker = false;
int s = rows;
int r = 0;

```

```

// Joins the vertex using beginShape()

```

```

for(int j = p; j >=0; j = j - 1){
  int t = 0;

```

```

  for(int i = coloumns-1; i >= 0 ; i = i - 1){

```

```

beginShape();

if(j % 2 == 0){

color1(i,t,r);
vertex(((i+5)*scl+150/2), (s*scale+50) , a1.get(a1.size()-(coloumns-i)-t-
r*2*coloumns)/scaling);

stroke(0);

color2(i,t,r);
vertex(((i+5)*scl+150/2), (s*scale-50) , b1.get(b1.size()-(coloumns-i)-t-
r*2*coloumns)/scaling);
color3(i,t,r);
vertex(((i+5)*scl+50/2), (s*scale-50) , b1.get(b1.size()-(coloumns-i+1)-t-
r*2*coloumns)/scaling);
color4(i,t,r);
vertex(((i+5)*scl+50/2), (s*scale+50) , a1.get(a1.size()-(coloumns-i+1)-t-
r*2*coloumns)/scaling);

checker = false;
t = t+1;
endShape();
}

else{

color5(i,t,r);
vertex(((i+5)*scl+150/2), (s*scale+50) , b2.get(b2.size()-(coloumns-i)-t-
r*b2.size()/2)/scaling);

color6(i,t,r);
vertex(((i+5)*scl+150/2), (s*scale-50) , a2.get(a2.size()-(coloumns-i)-t-
r*b2.size()/2)/scaling);

color7(i,t,r);
vertex(((i+5)*scl+50/2), (s*scale-50) , a2.get(a2.size()-(coloumns-i+1)-t-
r*b2.size()/2)/scaling);

color8(i,t,r);
vertex(((i+5)*scl+50/2), (s*scale+50) , b2.get(b2.size()-(coloumns-i+1)-t-
r*b2.size()/2)/scaling);

```



```

    t = t+1;
    checker = true;
    endShape();
  }

}

if(checker == true){
  r = r+1;
}
s = s-1;
}
}

//Defines color for a specific range of distance
void color1(int i,int t,int r){
  if(a1.get(a1.size()-(coloumns-i)-t-r*2*coloumns)>=0 && a1.get(a1.size()-(coloumns-i)-t-
r*2*coloumns)<30){
    fill(147,112,219);
  }
  else if(a1.get(a1.size()-(coloumns-i)-t-r*2*coloumns)>=30 && a1.get(a1.size()-(coloumns-i)-t-
r*2*coloumns)<60){
    fill(135,206,235);
  }
  else if(a1.get(a1.size()-(coloumns-i)-t-r*2*coloumns)>=60 && a1.get(a1.size()-(coloumns-i)-t-
r*2*coloumns)<90){
    fill(50,205,50);
  }
  else if(a1.get(a1.size()-(coloumns-i)-t-r*2*coloumns)>=90 && a1.get(a1.size()-(coloumns-i)-t-
r*2*coloumns)<120){
    fill(255,255,0);
  }
  else if(a1.get(a1.size()-(coloumns-i)-t-r*2*coloumns)>=120 && a1.get(a1.size()-(coloumns-i)-t-
r*2*coloumns)<150){
    fill(255,165,0);
  }
  else{
    fill(139,0,0);
  }
}
}
}

```

```

//Defines color for a specific range of distance
void color2(int i,int t,int r){
  if(b1.get(b1.size()-(coloumns-i)-t-r*2*coloumns)>=0 && b1.get(b1.size()-(coloumns-i)-t-
r*2*coloumns)<30){
    fill(147,112,219);
  }
  else if(b1.get(b1.size()-(coloumns-i)-t-r*2*coloumns)>=30 && b1.get(b1.size()-(coloumns-i)-t-
r*2*coloumns)<60){
    fill(135,206,235);
  }
  else if(b1.get(b1.size()-(coloumns-i)-t-r*2*coloumns)>=60 && b1.get(b1.size()-(coloumns-i)-t-
r*2*coloumns)<90){
    fill(50,205,50);
  }
  else if(b1.get(b1.size()-(coloumns-i)-t-r*2*coloumns)>=90 && b1.get(b1.size()-(coloumns-i)-t-
r*2*coloumns)<120){
    fill(255,255,0);
  }
  else if(b1.get(b1.size()-(coloumns-i)-t-r*2*coloumns)>=120 && b1.get(b1.size()-(coloumns-i)-
t-r*2*coloumns)<150){
    fill(255,165,0);
  }
  else{
    fill(139,0,0);
  }
}

```

```

//Defines color for a specific range of distance
void color3(int i,int t,int r){
  if(b1.get(b1.size()-(coloumns-i+1)-t-r*2*coloumns)>=0 && b1.get(b1.size()-(coloumns-i+1)-t-
r*2*coloumns)<30){
    fill(147,112,219);
  }
  else if(b1.get(b1.size()-(coloumns-i+1)-t-r*2*coloumns)>=30 && b1.get(b1.size()-(coloumns-
i+1)-t-r*2*coloumns)<60){
    fill(135,206,235);
  }
  else if(b1.get(b1.size()-(coloumns-i+1)-t-r*2*coloumns)>=60 && b1.get(b1.size()-(coloumns-
i+1)-t-r*2*coloumns)<90){
    fill(50,205,50);
  }
}

```

```

else if(b1.get(b1.size()-(coloumns-i+1)-t-r*2*coloumns)>=90 && b1.get(b1.size()-(coloumns-
i+1)-t-r*2*coloumns)<120){
    fill(255,255,0);
}
else if(b1.get(b1.size()-(coloumns-i+1)-t-r*2*coloumns)>=120 && b1.get(b1.size()-(coloumns-
i+1)-t-r*2*coloumns)<150){
    fill(255,165,0);
}
else{
    fill(139,0,0);
}
}
}

```

```

//Defines color for a specific range of distance
void color4(int i,int t,int r){
    if(a1.get(a1.size()-(coloumns-i+1)-t-r*2*coloumns)>=0 && a1.get(a1.size()-(coloumns-i+1)-t-
r*2*coloumns)<30){
        fill(147,112,219);
    }
    else if(a1.get(a1.size()-(coloumns-i+1)-t-r*2*coloumns)>=30 && a1.get(a1.size()-(coloumns-
i+1)-t-r*2*coloumns)<60){
        fill(135,206,235);
    }
    else if(a1.get(a1.size()-(coloumns-i+1)-t-r*2*coloumns)>=60 && a1.get(a1.size()-(coloumns-
i+1)-t-r*2*coloumns)<90){
        fill(50,205,50);
    }
    else if(a1.get(a1.size()-(coloumns-i+1)-t-r*2*coloumns)>=90 && a1.get(a1.size()-(coloumns-
i+1)-t-r*2*coloumns)<120){
        fill(255,255,0);
    }
    else if(a1.get(a1.size()-(coloumns-i+1)-t-r*2*coloumns)>=120 && a1.get(a1.size()-(coloumns-
i+1)-t-r*2*coloumns)<150){
        fill(255,165,0);
    }
    else{
        fill(139,0,0);
    }
}
}
}

```

```

//Defines color for a specific range of distance
void color5(int i,int t,int r){
  if(b2.get(b2.size()-(coloumns-i)-t-r*b2.size()/2)>=0 && b2.get(b2.size()-(coloumns-i)-t-
r*b2.size()/2)<30){
    fill(147,112,219);
  }
  else if(b2.get(b2.size()-(coloumns-i)-t-r*b2.size()/2)>=30 && b2.get(b2.size()-(coloumns-i)-t-
r*b2.size()/2)<60){
    fill(135,206,235);
  }
  else if(b2.get(b2.size()-(coloumns-i)-t-r*b2.size()/2)>=60 && b2.get(b2.size()-(coloumns-i)-t-
r*b2.size()/2)<90){
    fill(50,205,50);
  }
  else if(b2.get(b2.size()-(coloumns-i)-t-r*b2.size()/2)>=90 && b2.get(b2.size()-(coloumns-i)-t-
r*b2.size()/2)<120){
    fill(255,255,0);
  }
  else if(b2.get(b2.size()-(coloumns-i)-t-r*b2.size()/2)>=120 && b2.get(b2.size()-(coloumns-i)-t-
r*b2.size()/2)<150){
    fill(255,165,0);
  }
  else{
    fill(139,0,0);
  }
}

```

```

//Defines color for a specific range of distance
void color6(int i,int t,int r){
  if(a2.get(a2.size()-(coloumns-i)-t-r*b2.size()/2)>=0 && a2.get(a2.size()-(coloumns-i)-t-
r*b2.size()/2)<30){
    fill(147,112,219);
  }
  else if(a2.get(a2.size()-(coloumns-i)-t-r*b2.size()/2)>=30 && a2.get(a2.size()-(coloumns-i)-t-
r*b2.size()/2)<60){
    fill(135,206,235);
  }
  else if(a2.get(a2.size()-(coloumns-i)-t-r*b2.size()/2)>=60 && a2.get(a2.size()-(coloumns-i)-t-
r*b2.size()/2)<90){
    fill(50,205,50);
  }
}

```

```

else if(a2.get(a2.size()-(coloumns-i)-t-r*b2.size()/2)>=90 && a2.get(a2.size()-(coloumns-i)-t-
r*b2.size()/2)<120){
    fill(255,255,0);
}
else if(a2.get(a2.size()-(coloumns-i)-t-r*b2.size()/2)>=120 && a2.get(a2.size()-(coloumns-i)-t-
r*b2.size()/2)<150){
    fill(255,165,0);
}
else{
    fill(139,0,0);
}
}
}

```

```

//Defines color for a specific range of distance
void color7(int i,int t,int r){
    if(a2.get(a2.size()-(coloumns-i+1)-t-r*b2.size()/2)>=0 && a2.get(a2.size()-(coloumns-i+1)-t-
r*b2.size()/2)<30){
        fill(147,112,219);
    }
    else if(a2.get(a2.size()-(coloumns-i+1)-t-r*b2.size()/2)>=30 && a2.get(a2.size()-(coloumns-
i+1)-t-r*b2.size()/2)<60){
        fill(135,206,235);
    }
    else if(a2.get(a2.size()-(coloumns-i+1)-t-r*b2.size()/2)>=60 && a2.get(a2.size()-(coloumns-
i+1)-t-r*b2.size()/2)<90){
        fill(50,205,50);
    }
    else if(a2.get(a2.size()-(coloumns-i+1)-t-r*b2.size()/2)>=90 && a2.get(a2.size()-(coloumns-
i+1)-t-r*b2.size()/2)<120){
        fill(255,255,0);
    }
    else if(a2.get(a2.size()-(coloumns-i+1)-t-r*b2.size()/2)>=120 && a2.get(a2.size()-(coloumns-
i+1)-t-r*b2.size()/2)<150){
        fill(255,165,0);
    }
    else{
        fill(139,0,0);
    }
}
}
}

```

```

//Defines color for a specific range of distance
void color8(int i,int t,int r){
  if(b2.get(b2.size()-(coloumns-i+1)-t-r*b2.size()/2)>=0 && b2.get(b2.size()-(coloumns-i+1)-t-r*b2.size()/2)<30){
    fill(147,112,219);
  }
  else if(b2.get(b2.size()-(coloumns-i+1)-t-r*b2.size()/2)>=30 && b2.get(b2.size()-(coloumns-i+1)-t-r*b2.size()/2)<60){
    fill(135,206,235);
  }
  else if(b2.get(b2.size()-(coloumns-i+1)-t-r*b2.size()/2)>=60 && b2.get(b2.size()-(coloumns-i+1)-t-r*b2.size()/2)<90){
    fill(50,205,50);
  }
  else if(b2.get(b2.size()-(coloumns-i+1)-t-r*b2.size()/2)>=90 && b2.get(b2.size()-(coloumns-i+1)-t-r*b2.size()/2)<120){
    fill(255,255,0);
  }
  else if(b2.get(b2.size()-(coloumns-i+1)-t-r*b2.size()/2)>=120 && b2.get(b2.size()-(coloumns-i+1)-t-r*b2.size()/2)<150){
    fill(255,165,0);
  }
  else{
    fill(139,0,0);
  }
}

```

//Creates the spectrum for the range of different colors

```

void spectrum(){
  textSize(45);
  fill(0,0,128);
  text("Spectrum",65,680);
  fill(147,112,219);
  textSize(25);
  rect(75,700,20,20);
  text("Distance ∞ -> 50 m",97,719);

  fill(135,206,235);
  rect(75,730,20,20);
  text("Distance 49 -> 40 m",97,749);

  fill(50,205,50);

```

```

rect(428,700,20,20);
text("Distance 39 -> 30 m",450,719);

fill(255,255,0);
rect(428,730,20,20);
text("Distance 29 -> 20 m",450,749);

fill(255,165,0);
rect(791,700,20,20);
text("Distance 19 -> 10 m",813,719);

fill(240,71,71);
rect(791,730,20,20);
text("Distance 9 -> 0 m",813,749);
}

```

### Code Bibliography:

- 1) (n.d.). Retrieved October 27, 2016, from <https://forum.arduino.cc/index.php?topic=243076.0>
- 2) Measure Distance with a Sonar Sensor on an Arduino. (n.d.). Retrieved from <https://www.allaboutcircuits.com/projects/measure-distance-with-a-sonar-sensor-on-an-arduino/>
- 3) Stamigni D. (2010). Arduino & Ultrasonic Sensor (MB1040 LV-MaxSonar-EZ4 by MaxBotix. Retrieved from [https://www.youtube.com/watch?v=C7kOmo-b\\_Ko](https://www.youtube.com/watch?v=C7kOmo-b_Ko)
- 2) Processing for Android. (n.d.). Retrieved from <http://android.processing.org/tutorials/sensors/index.html>
- 3) Mithila. (2014). Tutorial : Ultrasonic Distance module HC - SR04 with Arduino and C#. Retrieved from <https://www.youtube.com/watch?v=7xCVSWVLRKg>
- 4) Wagle, S. (2016). Ultrasonic Map-Maker using an Arduino Yun - Hackster.io. Retrieved from <https://www.hackster.io/Satyavrat/ultrasonic-map-maker-using-an-arduino-yun-37c72e>
- 5) Larry. (2009). Arduino + Processing – 3D Sensor Data Visualisation — Lucky Larry. Retrieved from <http://luckylarry.co.uk/arduino-projects/arduino-processing-3d-sensor-data-visualisation/>
- 6) Coding Challenge #11: 3D Terrain Generation with Perlin Noise in Processing. (2016). Retrieved from <https://www.youtube.com/watch?v=IKB1hWWedMk>

### Block 3: MatLab Bode plot:

```
sys = tf([0.0032 0],[1 0.05656 2.0016 0.05656 1]);  
bode(sys)  
grid
```

### Block 4: MatLab Transducer Parameter Calculations:

```
% function [ fr,fa ] = Td0200ka_parameters( R1,L1,C1,Co,C,fs,fp )  
%R1(series Resistance), Co(Parallel Capacitance), C1(Series Capacitance),  
%L1(Series Inductance), fs(series Resonance), fp(parallel resonance)  
%fr(resonant frequency, fa(anti-resonant frequency),  
%Zs(transducer impedance at resonance),w(frequency), C(static Capacitance)  
%f1 ;f2(3dB from resonant frequency), Qm(Mechanical sharpness), Zr(resonant resistance)  
double fr; double fa; double Qm; double Zs;  
R1=353.384430;L1= 13.236637*10^(-3);C1=0.047358*10^(-9);Co=3.204421*10^(-  
9);C=1500*10^(-12);fs=201.024*10^(3);fp=204*10^(3);  
fr=1./(2*pi*(sqrt(L1*C1)));  
fa= 1./(2*pi*sqrt((L1*Co*C1)./C1+Co));  
% Qm=fr./(f2-f1);  
Qm=47.308;  
Zr= fa^2/((2*pi*fr*Qm*C*(fa^2-fr^2)));  
  
ws= 2*pi*fs;  
wp=2*pi*fp;  
%w=2;  
  
w=0:0.01:1300*1000;double Zs;  
% Transducer Impedance  
Zs=(1/w*Co)*((ws^2-w^2)+(1i*R1*w/L1))/((-R1*w/L1)+1i*(wp^2-w^2));  
disp(Zs)  
disp(Zr)  
disp(fr)  
disp(fa)  
  
% plot(w,Zs);  
% xlabel('frequency')  
% ylabel('Impedance')  
% title('Transducer Impedance Characteristics')  
% disp(Qm)  
% end
```



**Block 5: MatLab Maximum Power Theorem Curve:**

```
R=-3:0.01:3;
```

```
double P;  
Vavg=10;  
%double Vavg;  
P= Vavg*(2-R.^2);  
plot(P,'r');  
xlabel('Load Resistance');  
ylabel('Power across load');  
title('Po Vs R ');
```

**Block 6: MatLab Power Vs Current/ Voltage Characteristics:**

```
function [ Ep,Ip ] = Voltage_peak( P, Rp )  
double P;  
double Rp;  
  
%P=Ep.^2/(2*Rp)  
Ep=sqrt(P*2*Rp)./sqrt(2);  
figure(1)  
subplot(2,1,1)  
plot(P,Ep);  
xlabel('P-Power');  
ylabel('Voltage Ep');  
title('Voltage Vs Power');  
Ip=P./Ep;  
subplot(2,1,2)  
plot(P,Ip);  
xlabel('Power-P');  
ylabel('Current-I');  
title('Current Vs Power');  
  
end
```

```
[Vm,Im]=Voltage_peak( 0:0.1:40, 500 );  
% Voltage_peak( P, Rp )  
disp('Peak Voltage Ep: ')  
disp( Vm)  
disp('Peak Voltage Ep: ')  
disp(Im)
```

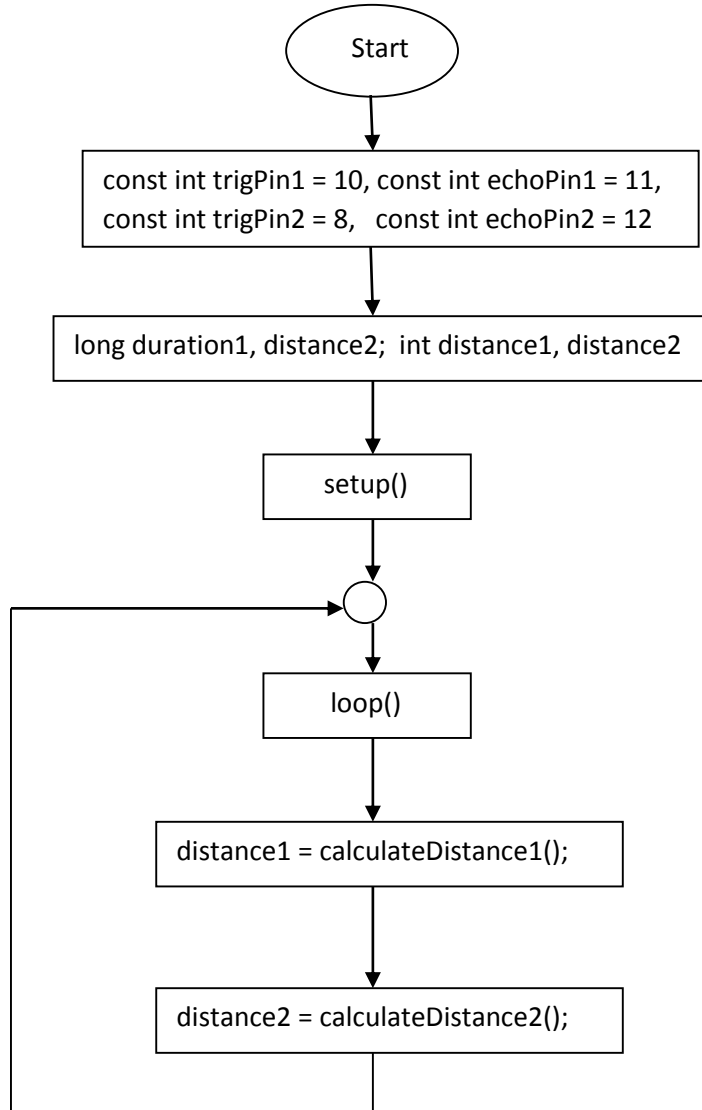
## Block 7: MatLab

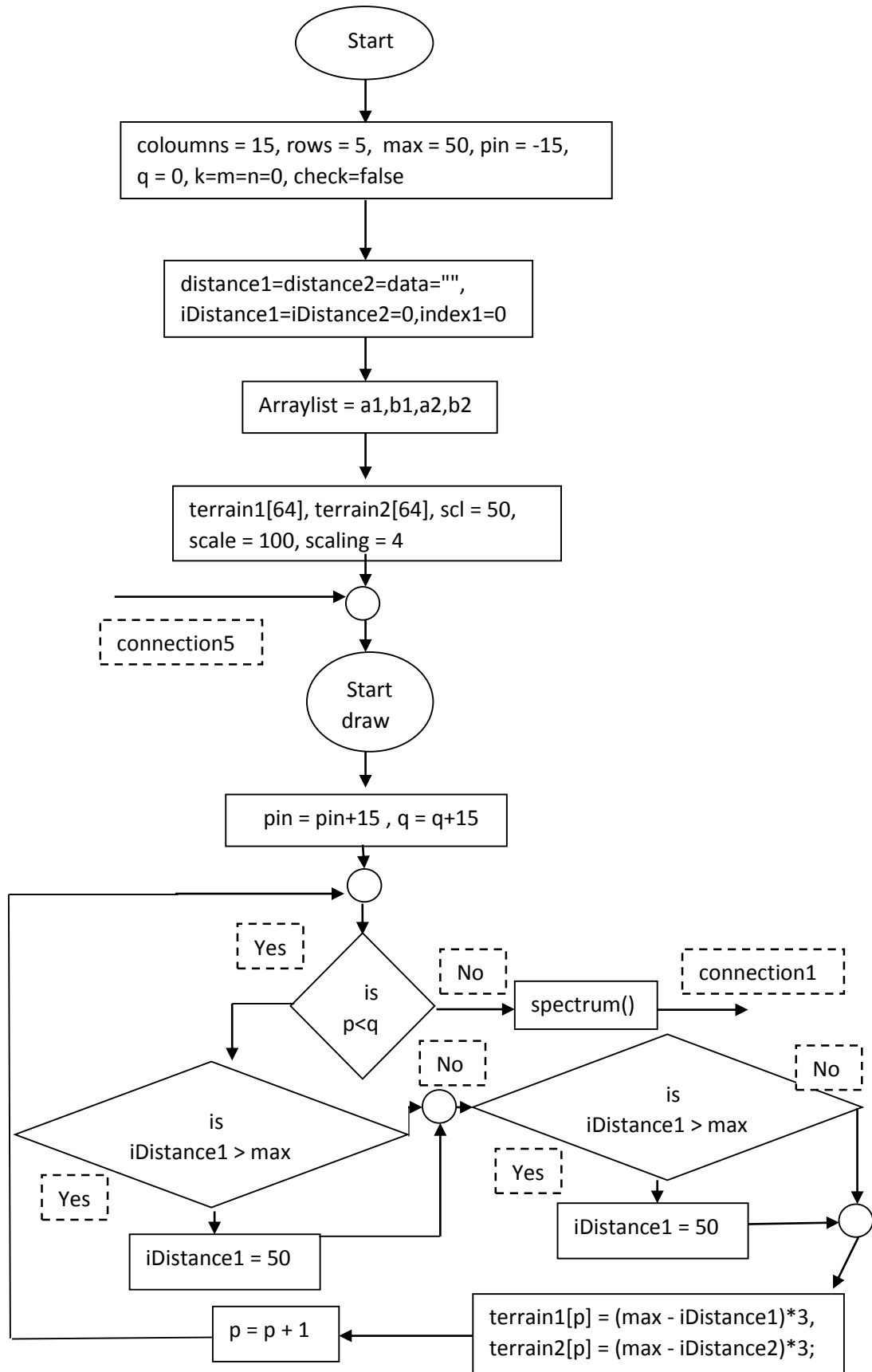
```
double Rs;
y= Rs.^2-500*Rs-(530.52).^2;

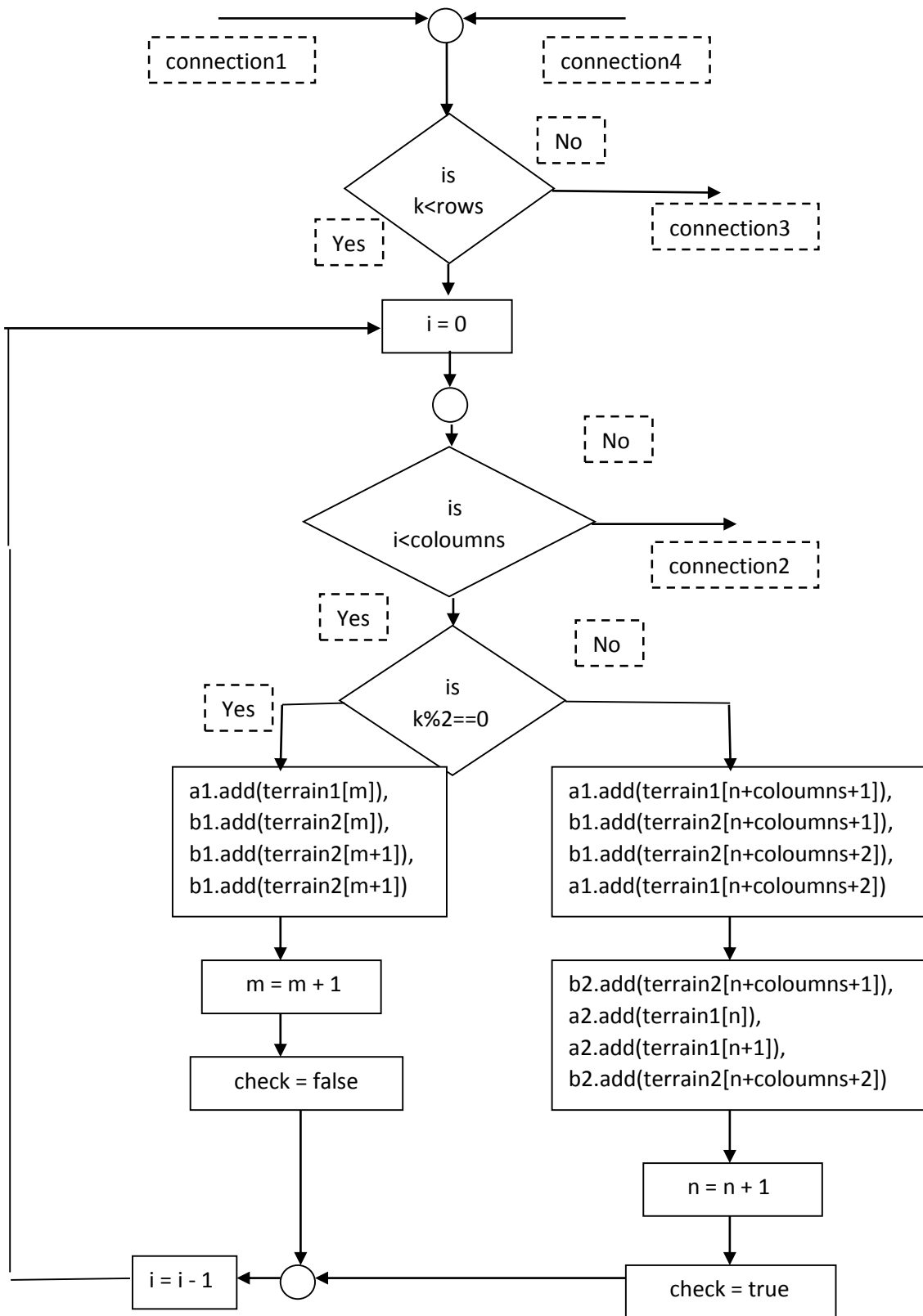
plot(Rs,y);
xlabel('Series Resistance');
ylabel('Impedance Characteristics');
title('Impedance Matching')
real(roots(y))
roots(y)

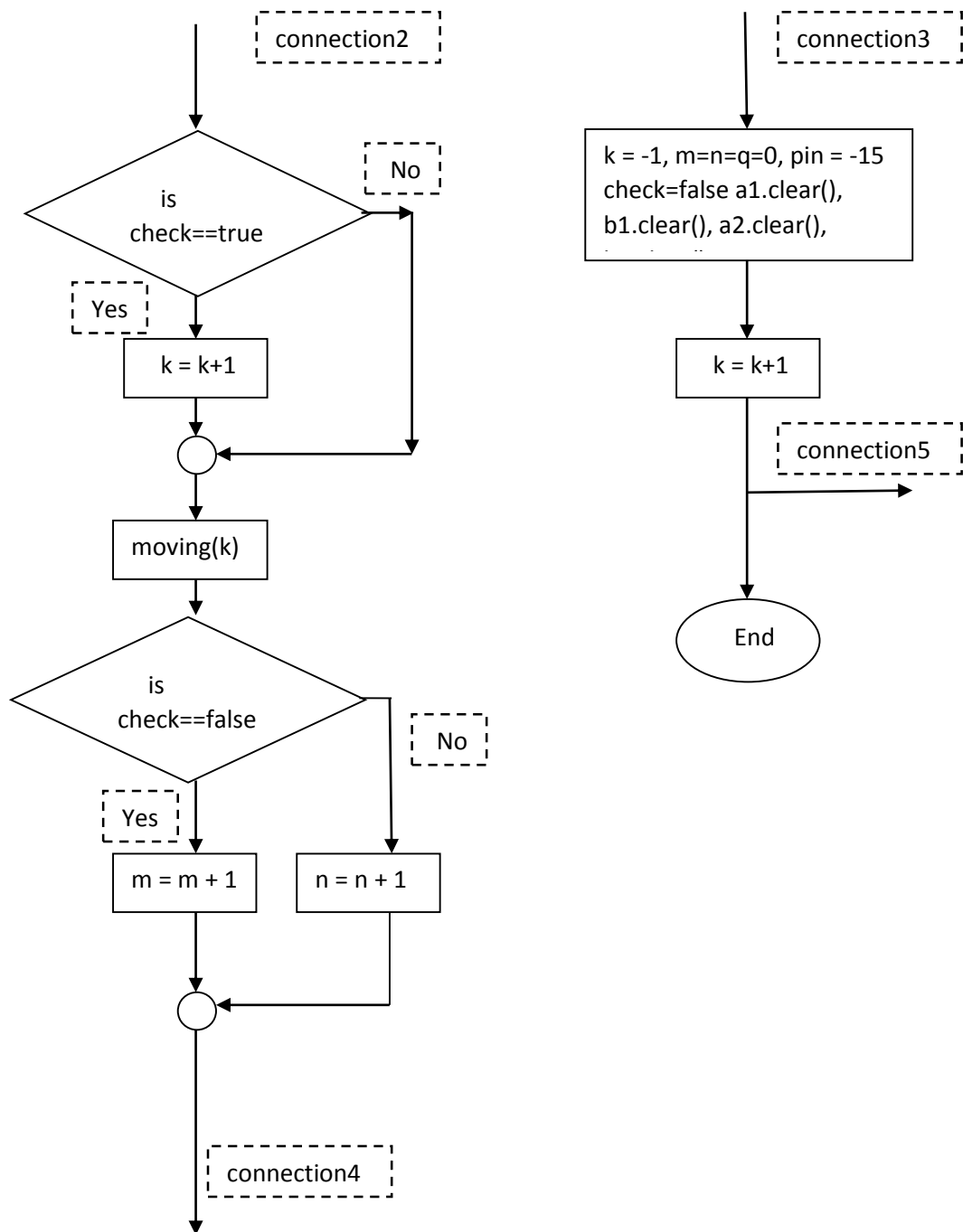
% z=[1 -500 -281451.5];
% roots(z)
% plot(z);
% figure(2)
% xlabel('Series Resistance');
% ylabel('Impedance Characteristics');
% title('Impedance Matching')
```

## Appendix E: Flow Charts

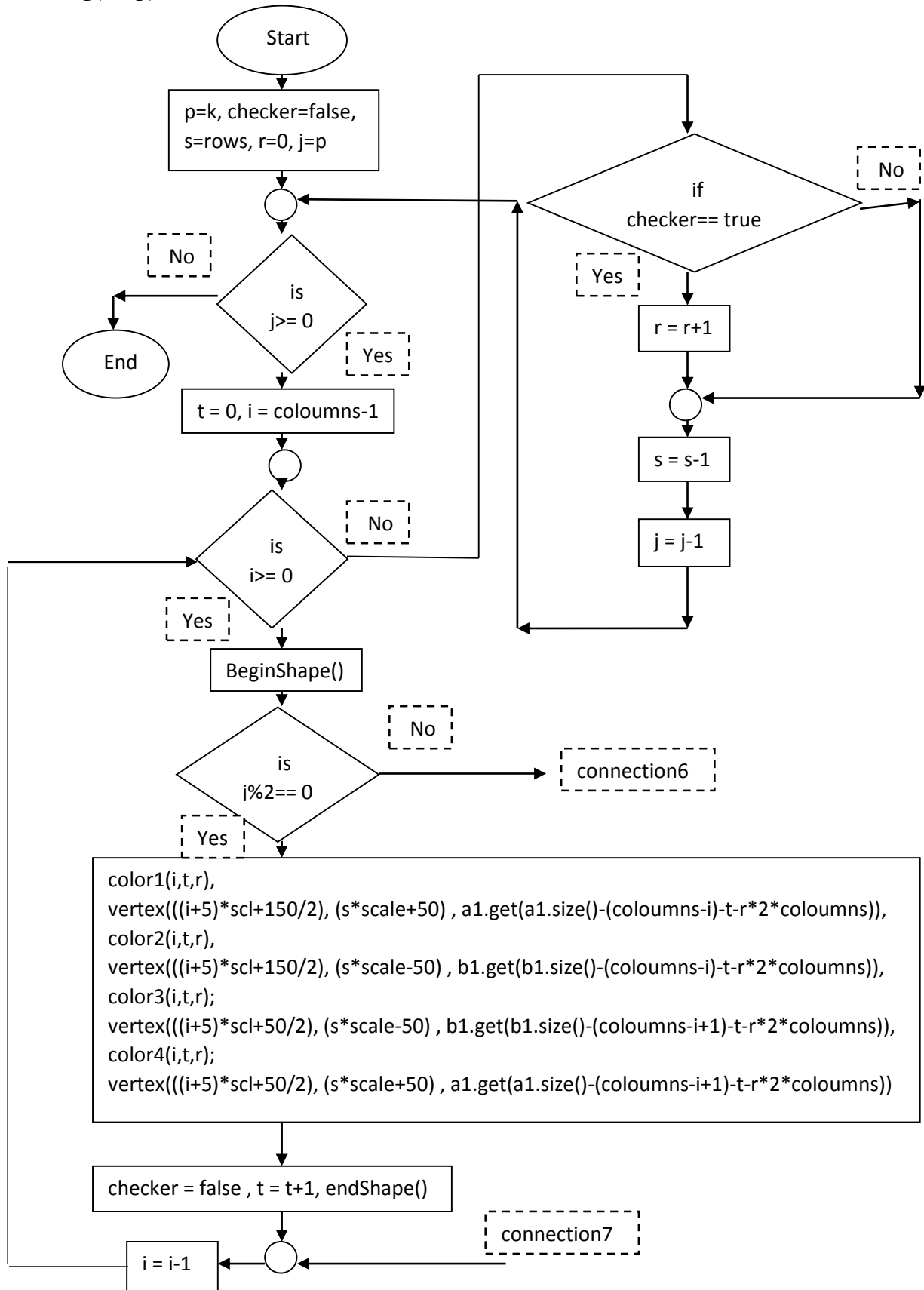


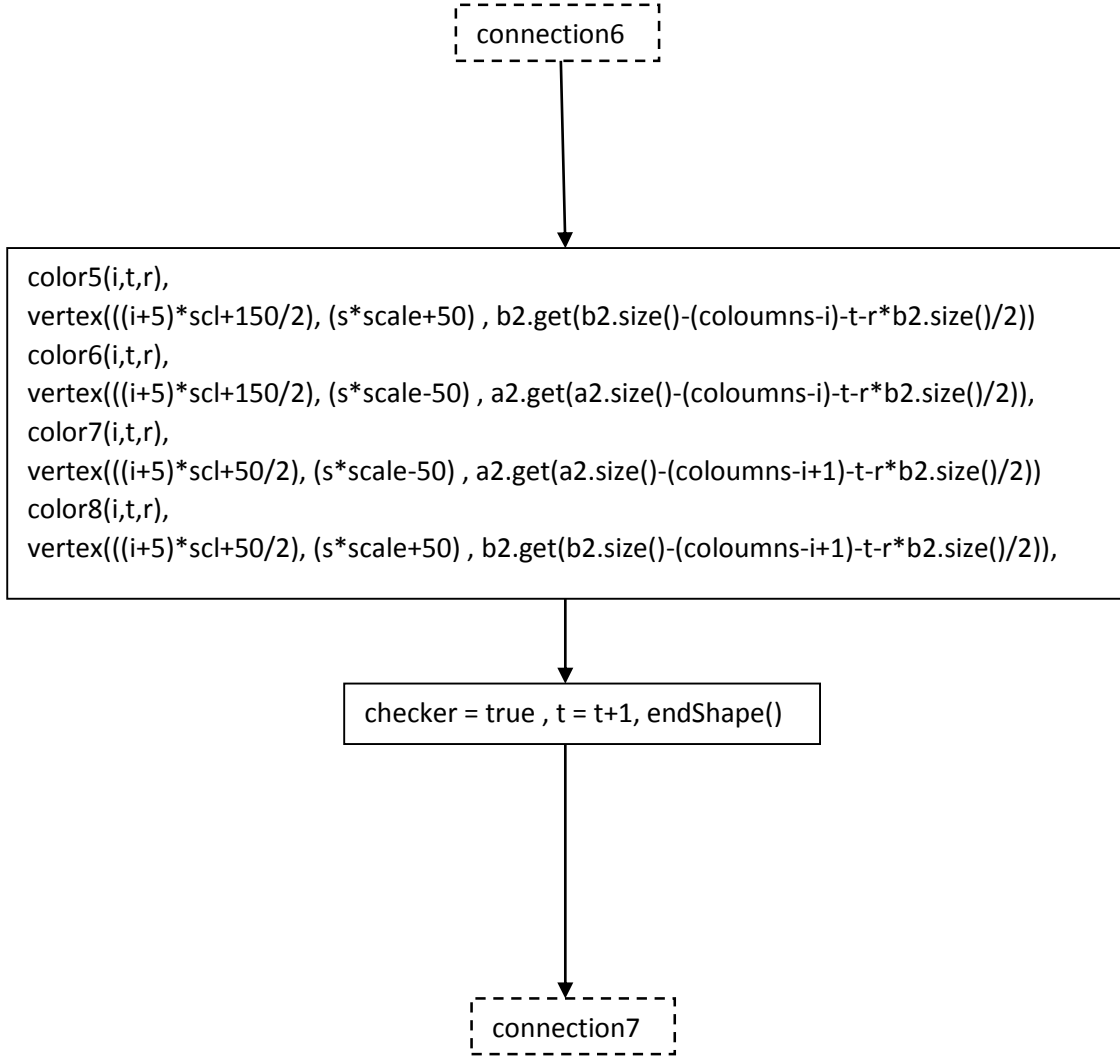






**void moving(int p) :**

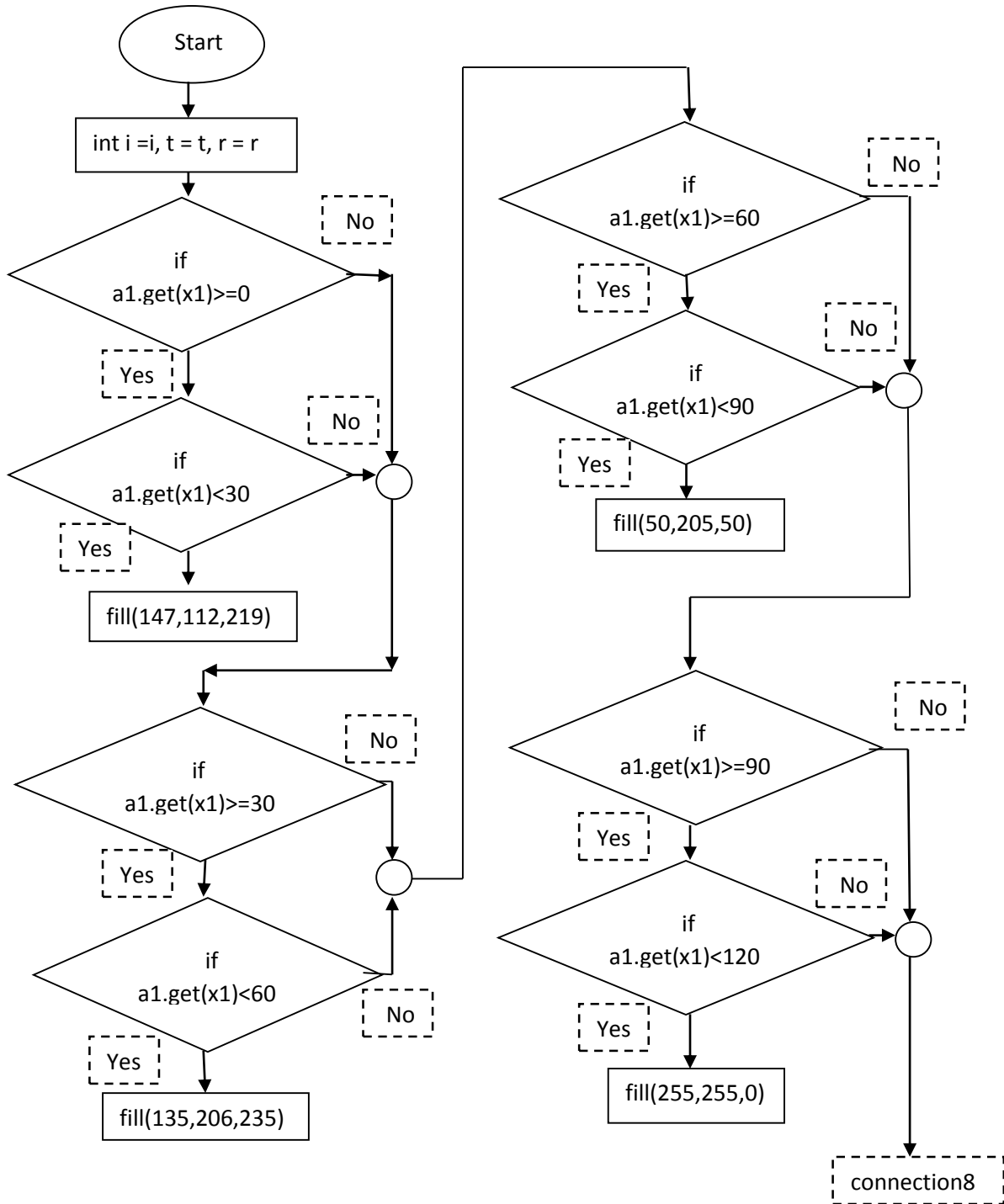


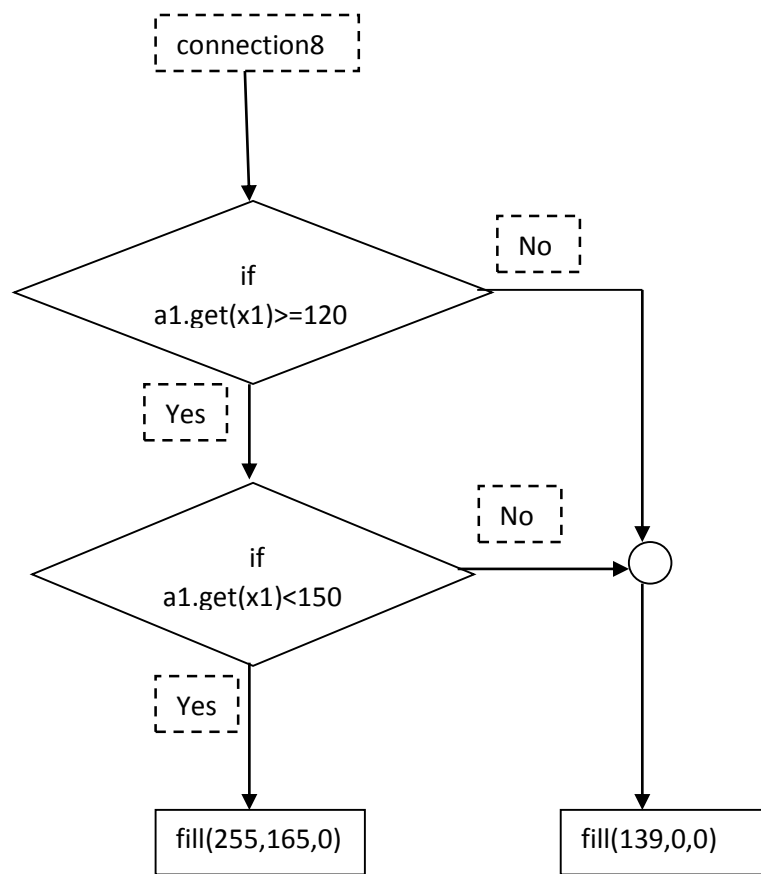




### Color1(int i, int t, int r)

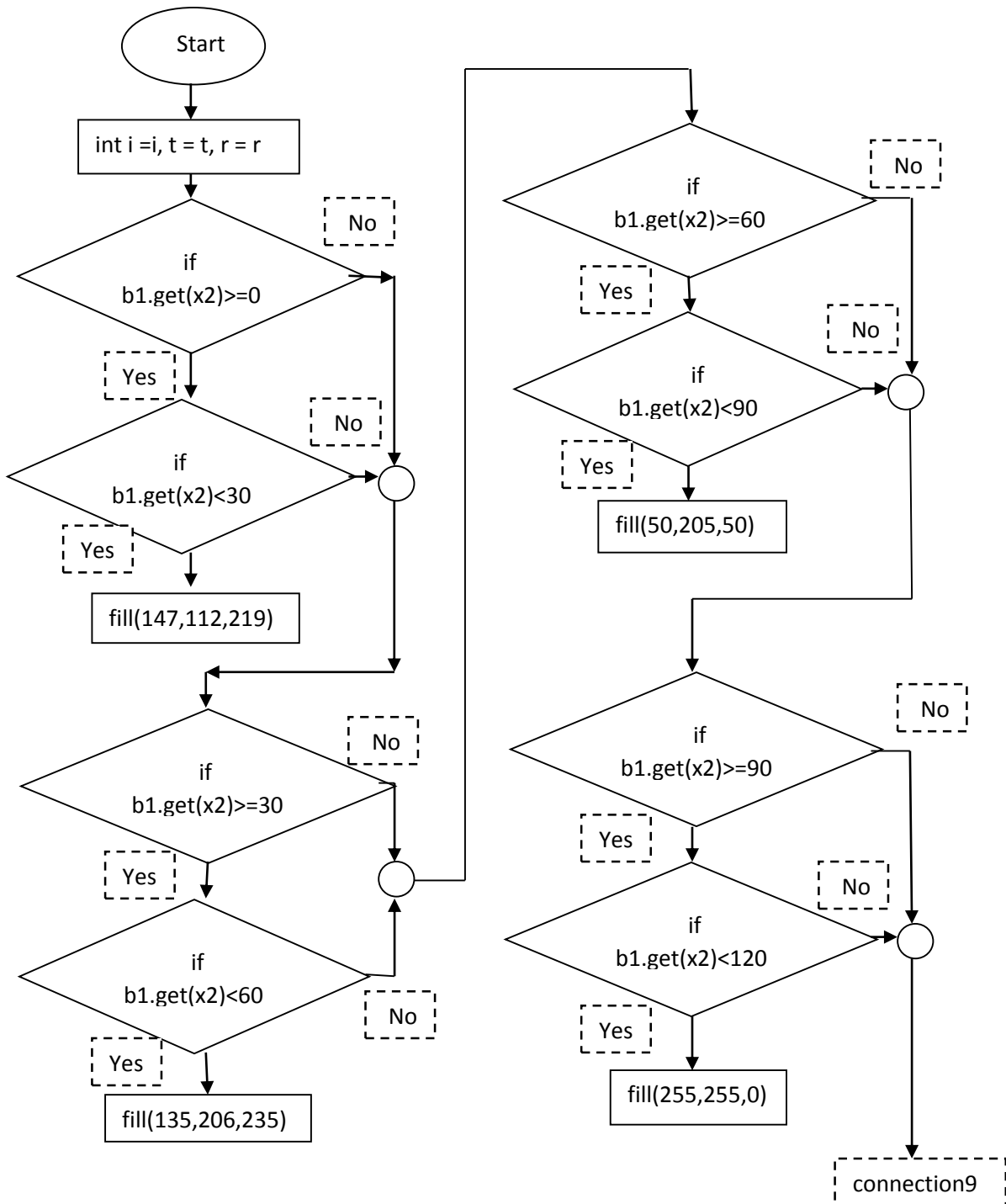
Here,  $x1 = a1.size() - (\text{columns} - i) - t - r * 2 * \text{columns}$

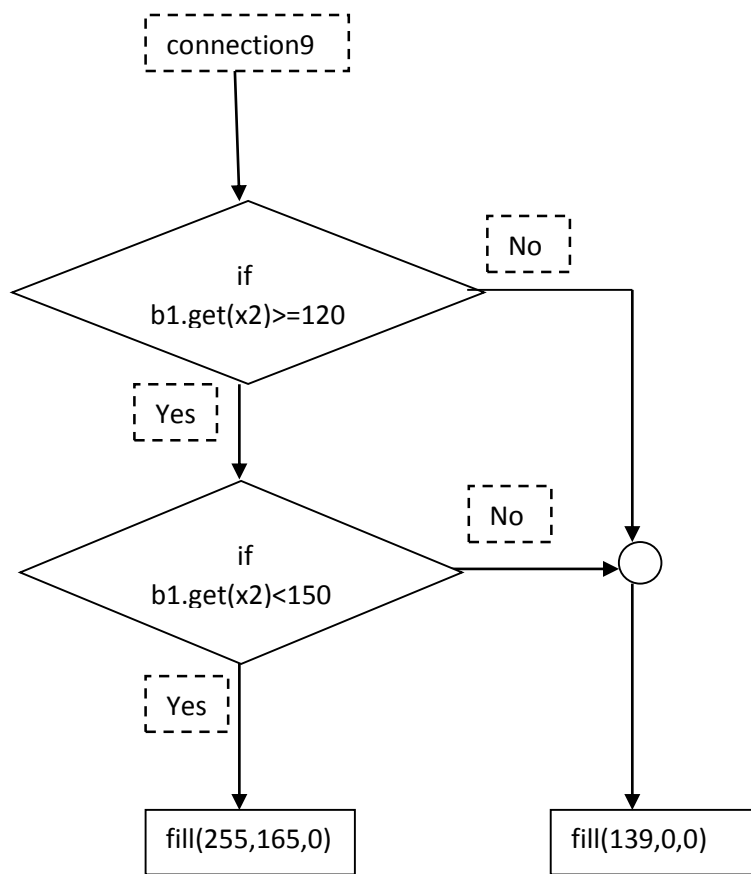




### Color2(int i, int t, int r)

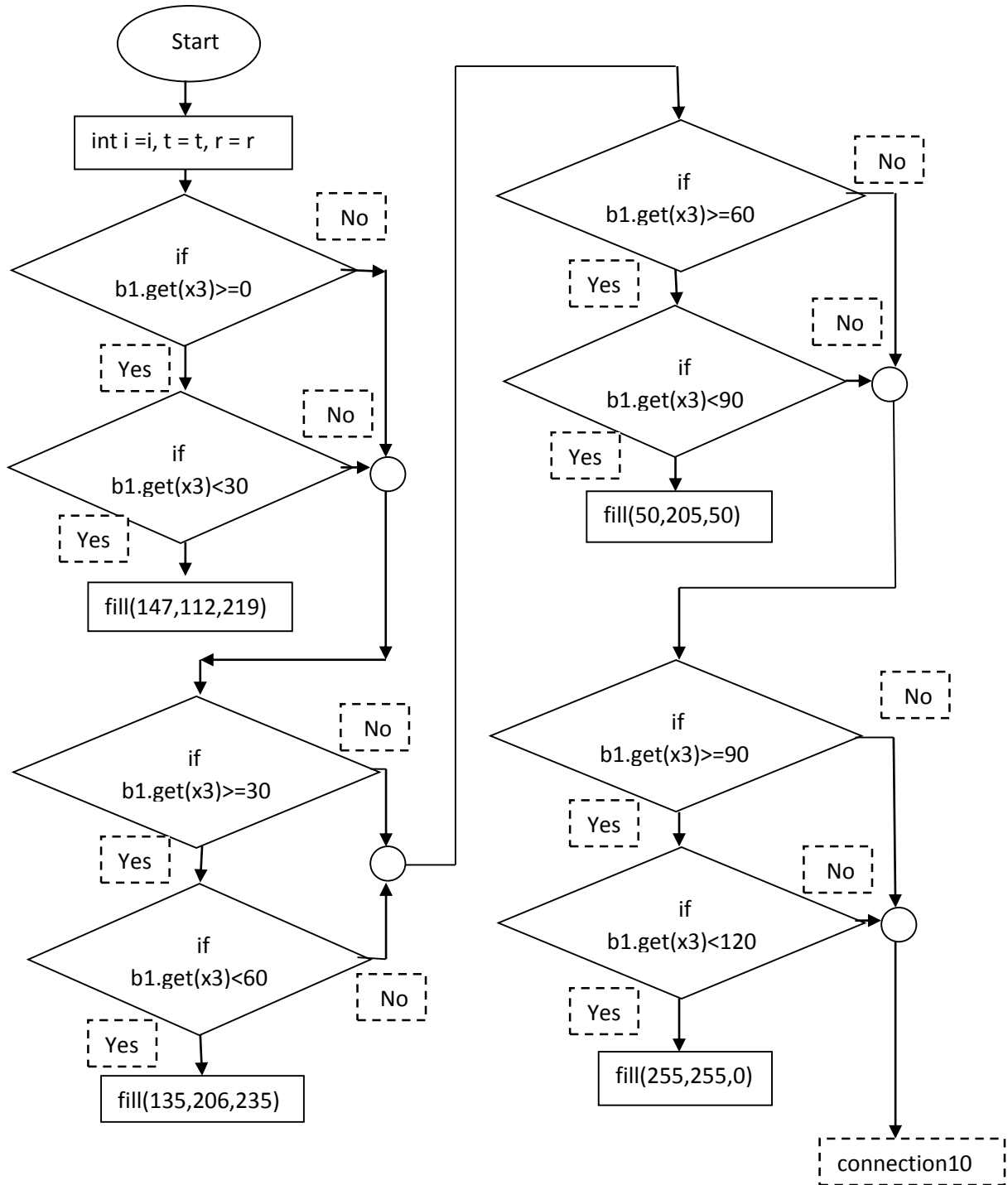
Here,  $x2 = b1.size() - (\text{columns} - i) - t - r * 2 * \text{columns}$

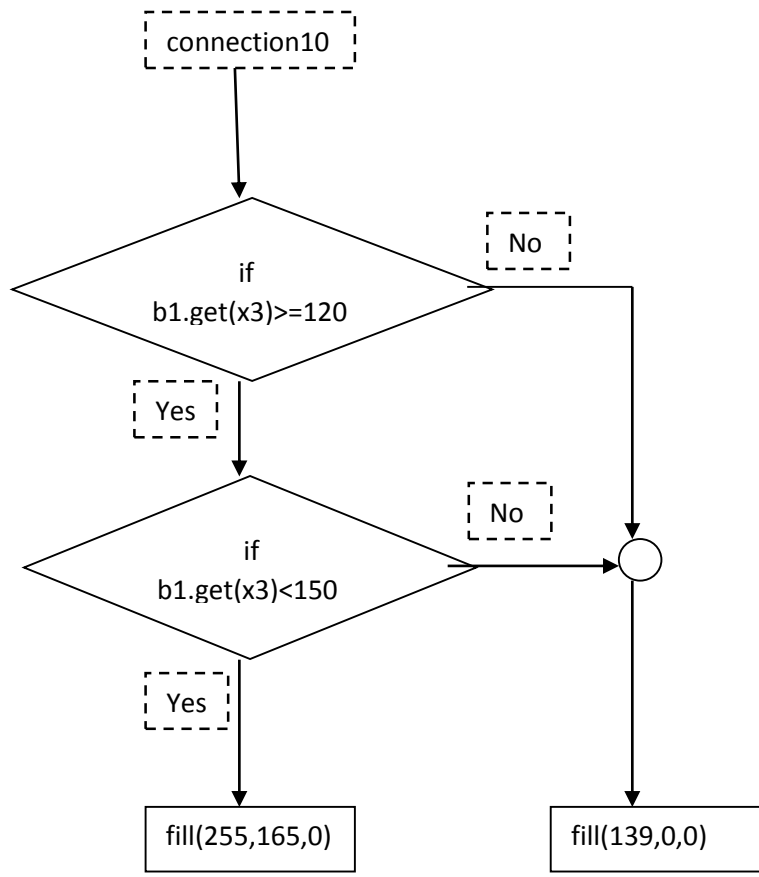




### Color3(int i, int t, int r)

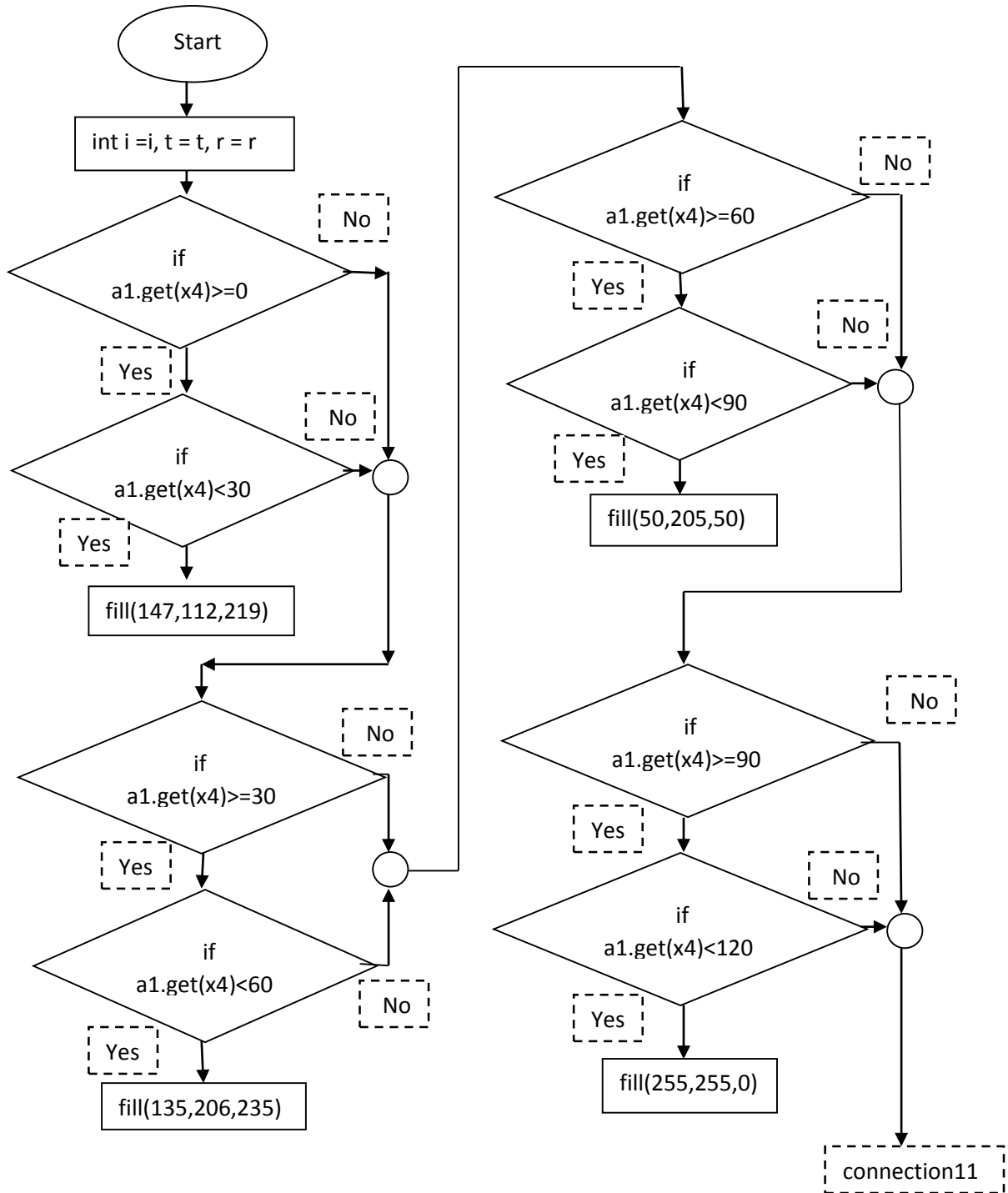
Here,  $x3 = b1.size() - (\text{coloumns} - i + 1) - t - r * 2 * \text{coloumns}$

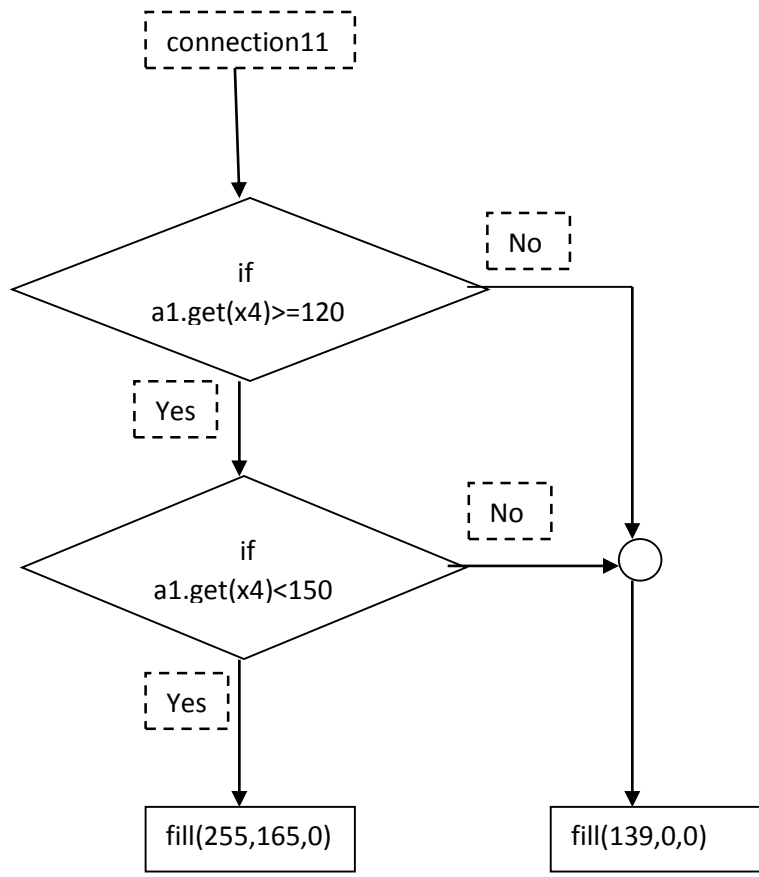




### Color4(int i, int t, int r)

Here,  $x4 = a1.size() - (\text{coloumns} - i + 1) - t - r * 2 * \text{coloumns}$

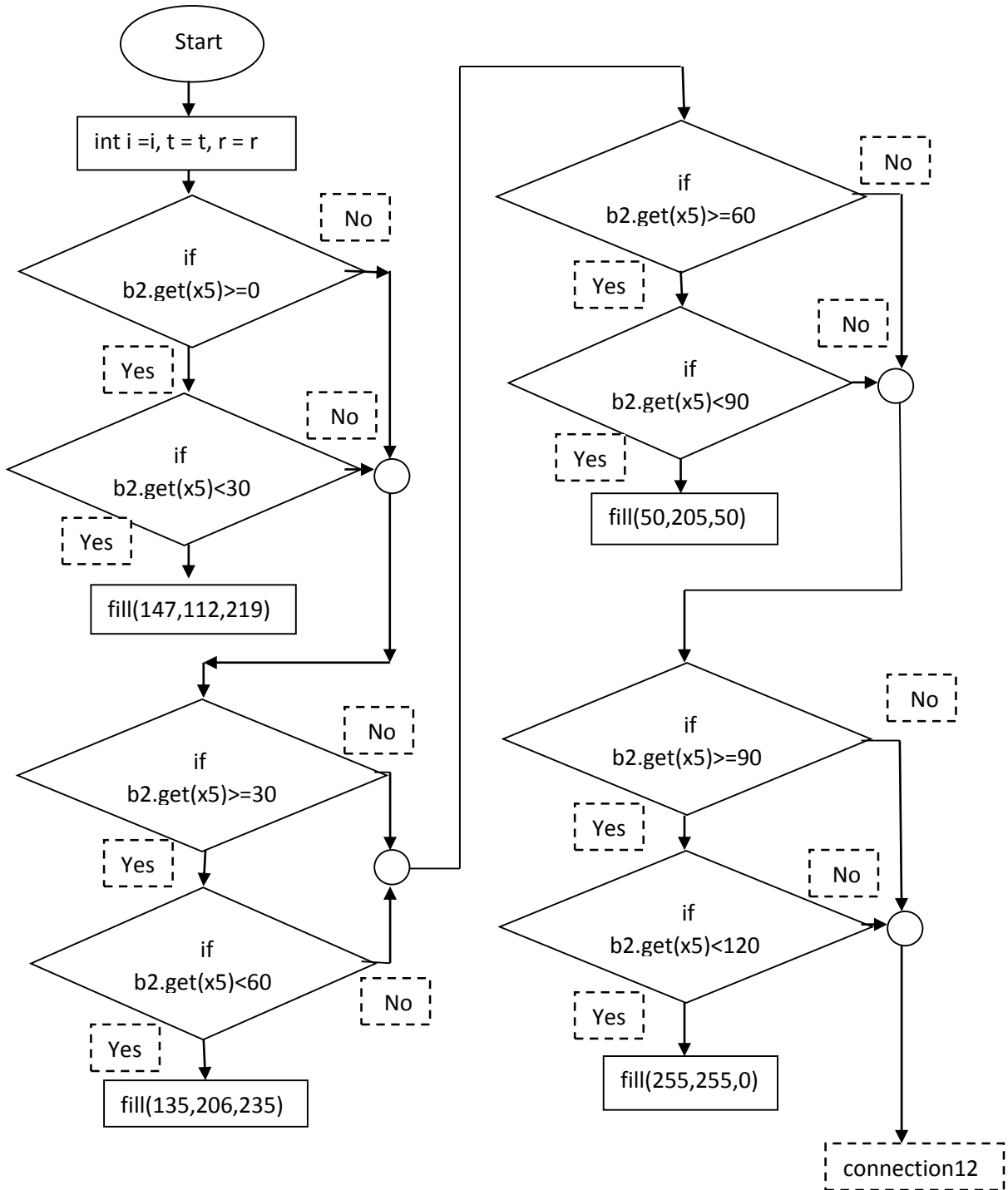


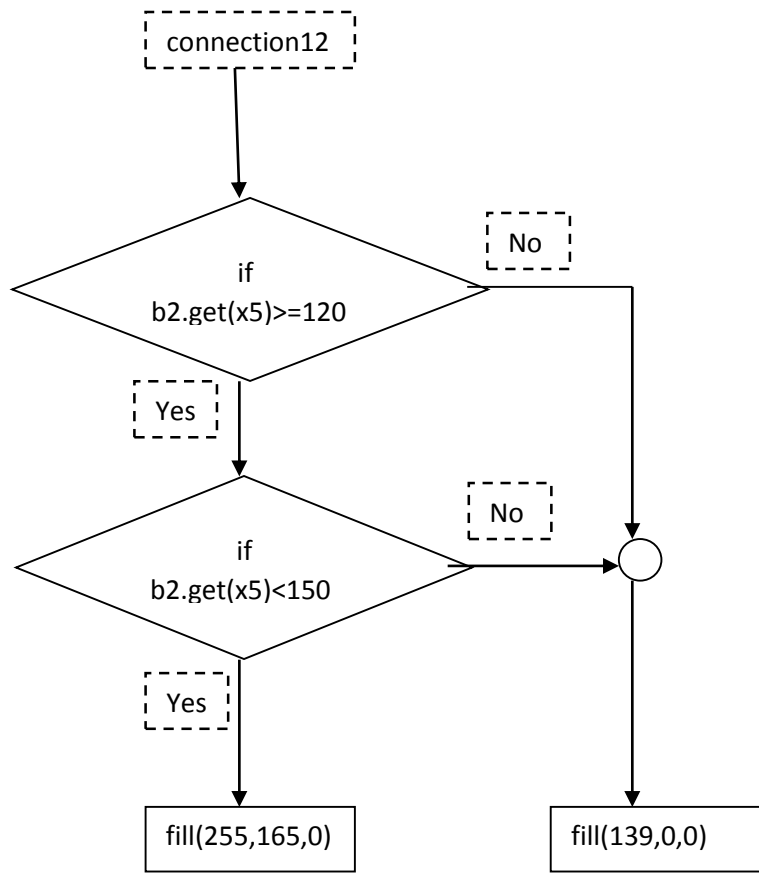




### Color5(int i, int t, int r)

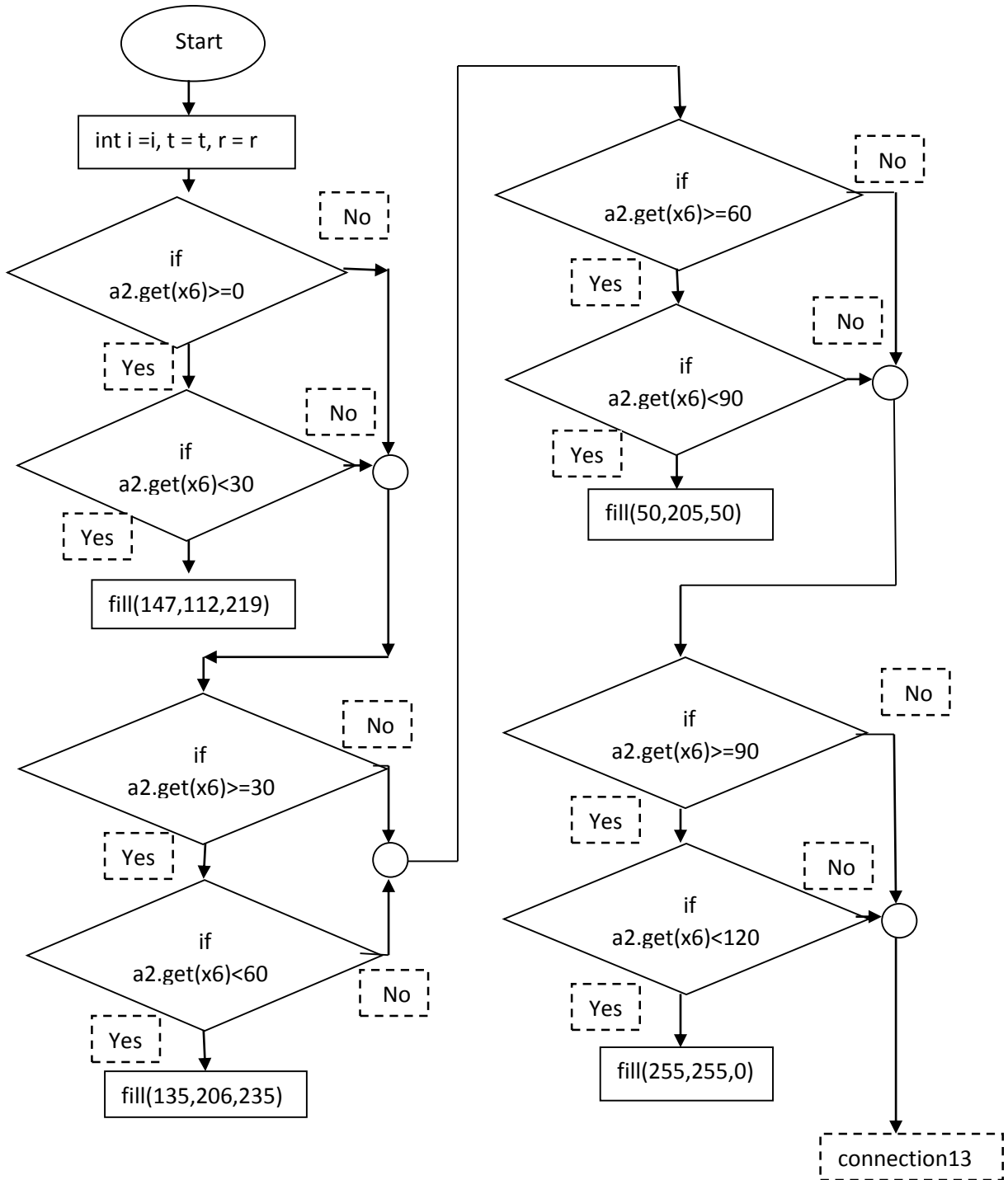
Here,  $x5 = b2.size() - (\text{coloumns} - i) - t - r * b2.size() / 2$

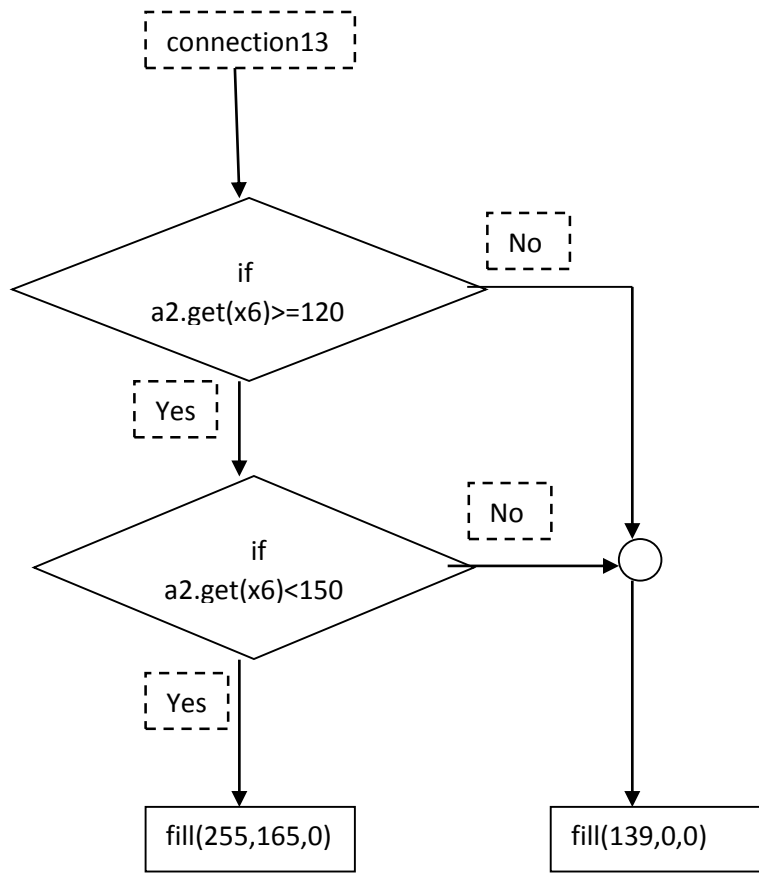




### Color6(int i, int t, int r)

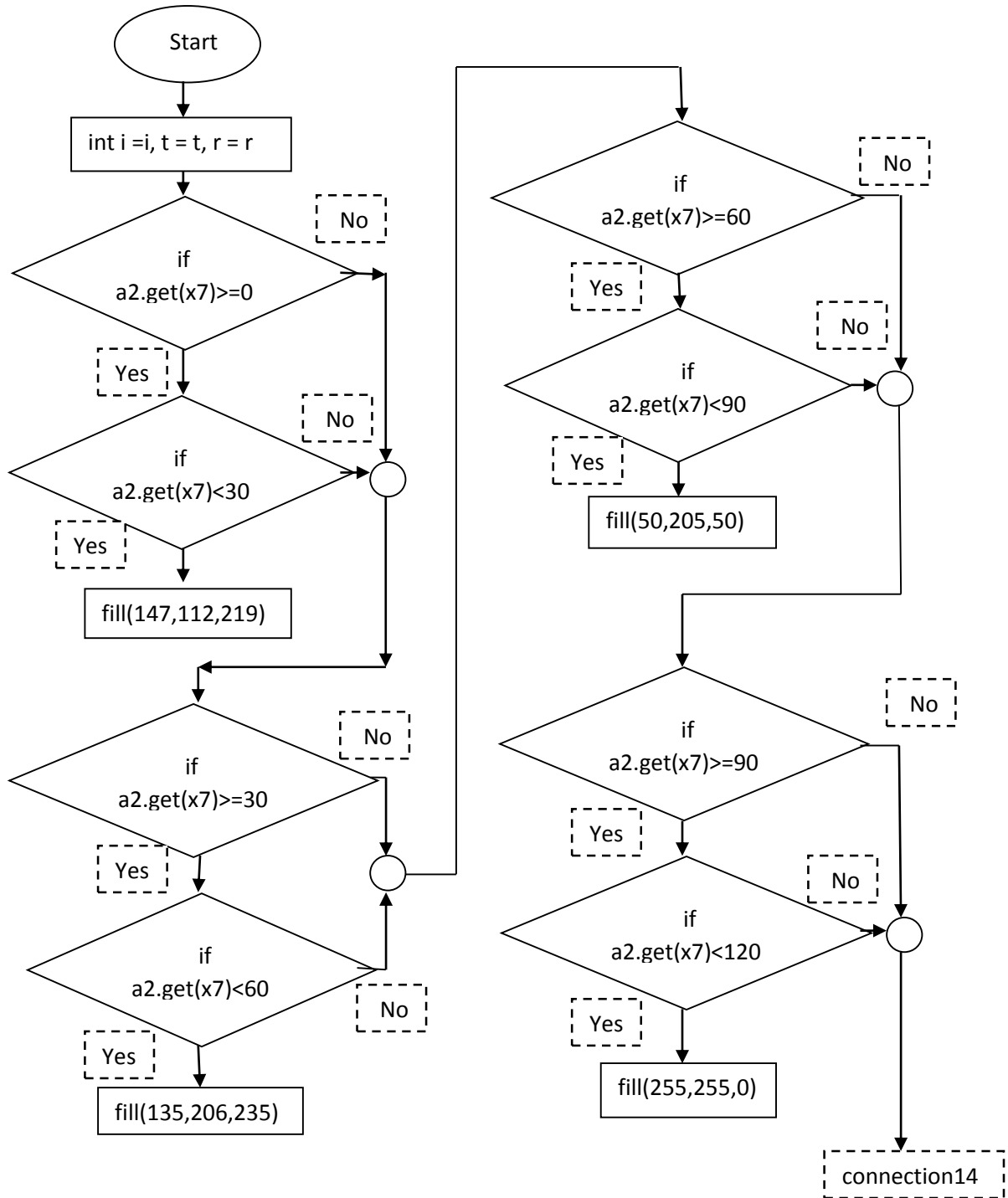
Here,  $x6 = a2.size() - (\text{coloumns} - i) - t - r * b2.size() / 2$

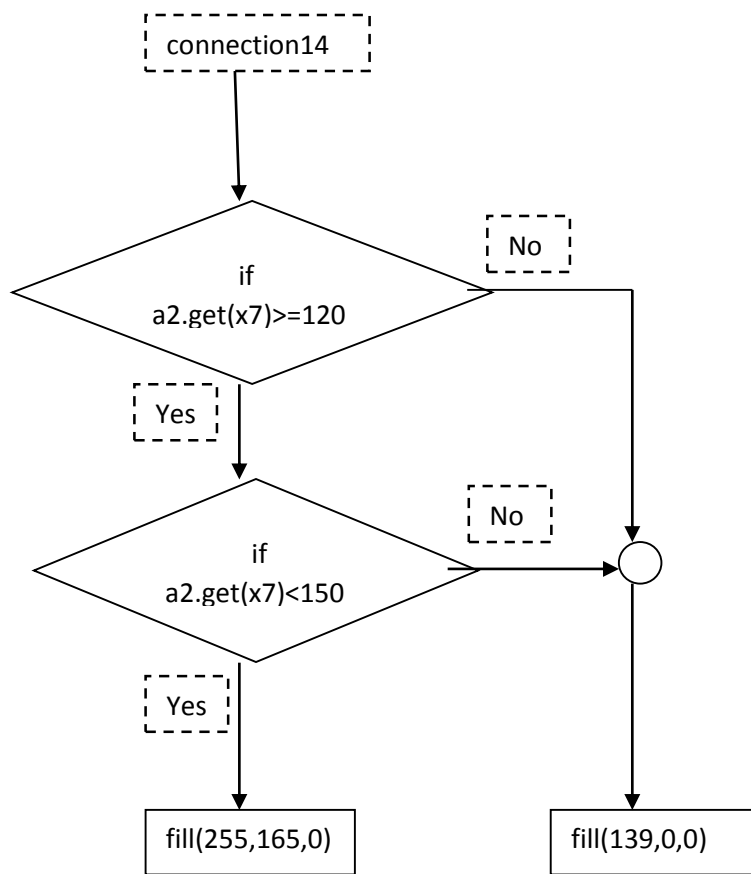




### Color7(int i, int t, int r)

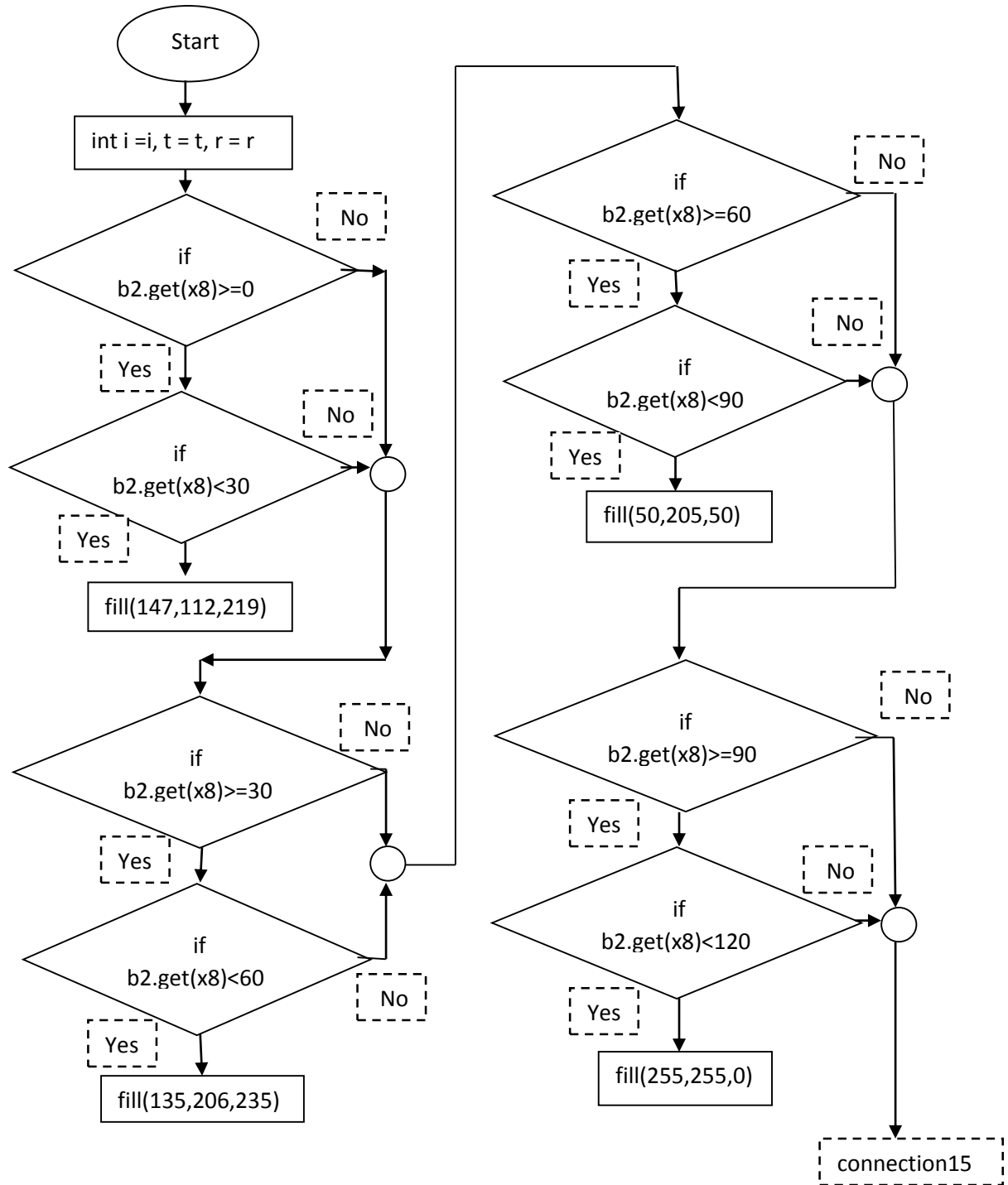
Here,  $x7 = a2.size() - (\text{coloumns} - i + 1) - t - r * b2.size() / 2$

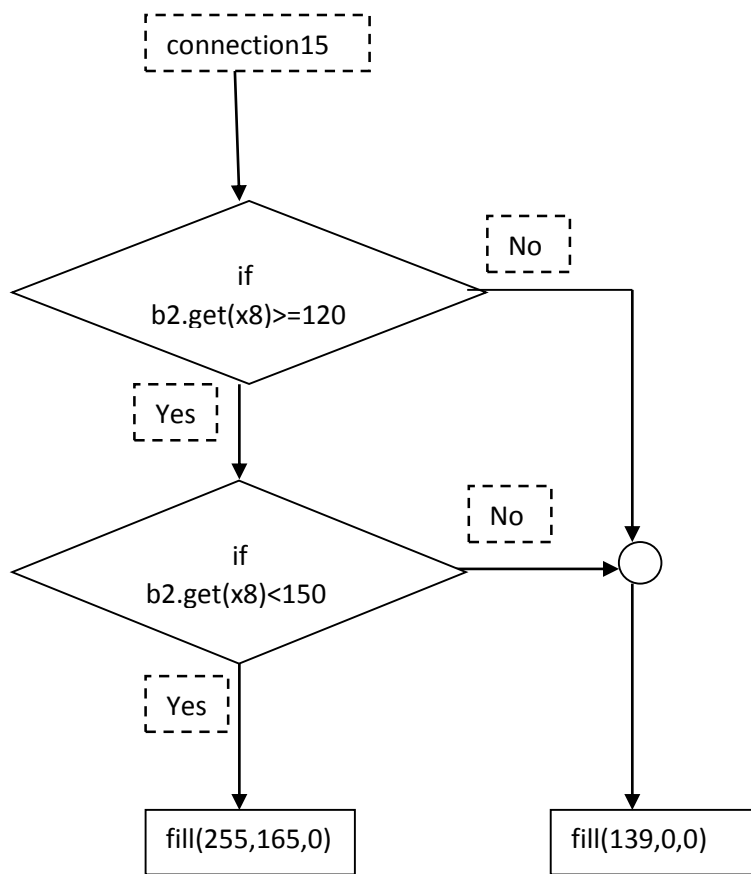




### Color8(int i, int t, int r)

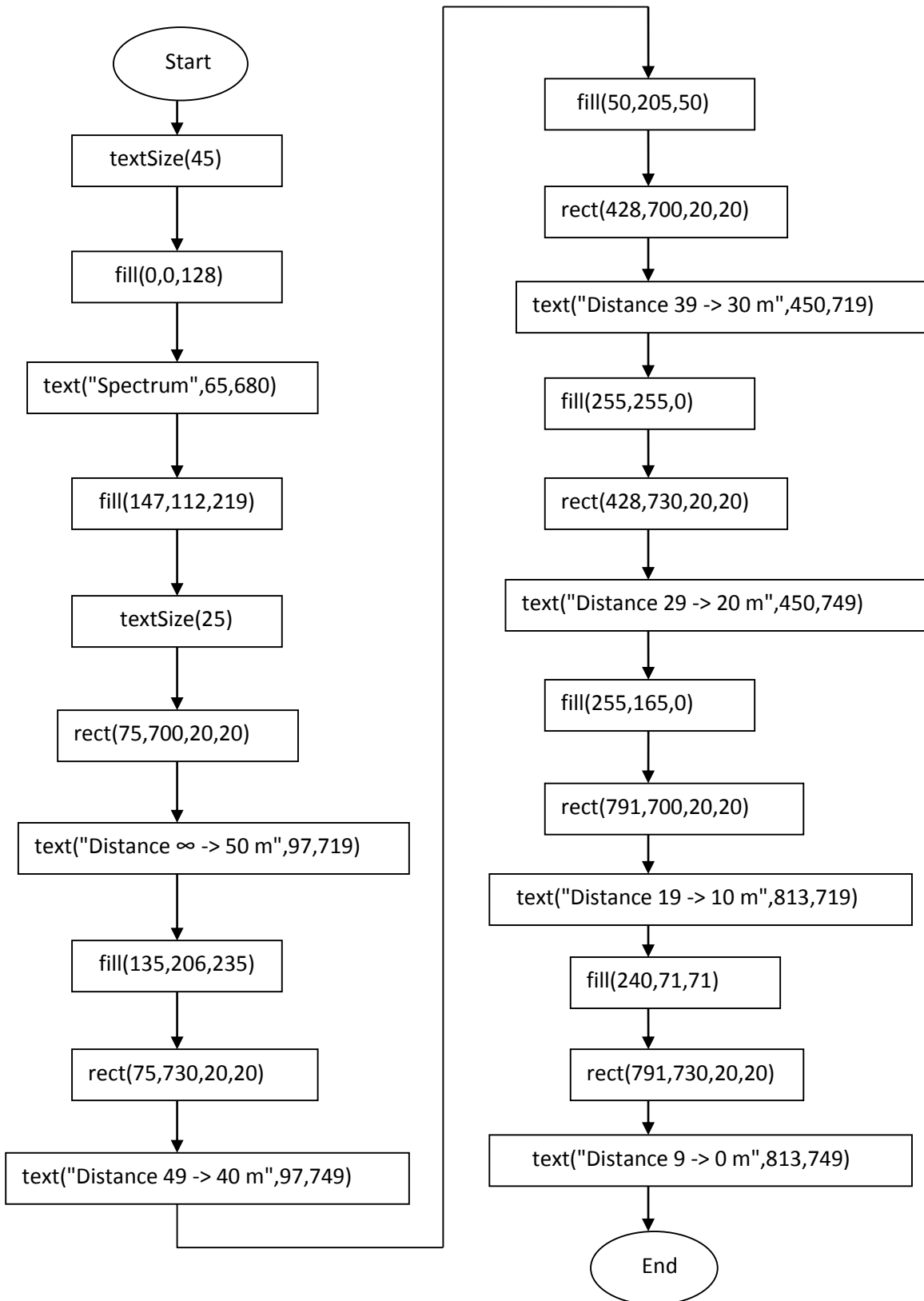
Here,  $x8 = b2.size() - (\text{coloumns} - i + 1) - t - r * b2.size() / 2$







spectrum()



**serialEvent(Serial myPort):**

